Department of Mechanical Engineering

Ground Source Heat Pumps (GSHP) and Underground Thermal Energy Storage (UTES) - Key Vectors to a Future Energy Transition

Oleg Todorov

Aalto University

DOCTORAL THESES

Aalto University publication series
DOCTORAL THESES 66/2022

Ground Source Heat Pumps (GSHP) and Underground Thermal Energy Storage (UTES) - Key Vectors to a Future Energy Transition

Oleg Todorov

A doctoral thesis completed for the degree of Doctor of Science (Technology) to be defended, with the permission of the Aalto University School of Engineering, at a public examination held at the lecture hall K1-216 of the school on 27 May 2022 at 12.00.

Aalto University
School of Engineering
Department of Mechanical Engineering
Energy Technology

Supervising professor
Associate Professor, HVAC technology Risto Kosonen, Aalto University, Finland

Thesis advisor
Senior University Lecturer, Docent, D.Sc. (Tech.) Kari Alanne, Aalto University, Finland

Preliminary examiners
Dr. José Acuña, Bengt Dahlgren Stockholm Geo AB, Sweden
Associate Professor Toke Rammer Nielsen, Technical University of Denmark

Opponent
Professor Thomas Olofsson, Umeå University, Sweden

Aalto University publication series
DOCTORAL THESES 66/2022

ISBN 978-952-64-0798-2 (printed)
ISBN 978-952-64-0799-9 (pdf)
ISSN 1799-4934 (printed)
ISSN 1799-4942 (pdf)
http://urn.fi/URN:ISBN:978-952-64-0799-9

Images: Cover Image: Mikko Raskinen / Aalto University

Unigrafia Oy
Helsinki 2022

Finland

Printed matter
4041-0619

Author
Oleg Todorov

Name of the doctoral thesis
Ground Source Heat Pumps (GSHP) and Underground Thermal Energy Storage (UTES) - Key Vectors to a Future Energy Transition

Publisher School of Engineering

Unit Department of Mechanical Engineering

Series Aalto University publication series DOCTORAL THESES 66/2022

Field of research Energy Technology

Manuscript submitted 15 February 2022 **Date of the defence** 27 May 2022

Permission for public defence granted (date) 28 April 2022 **Language** English

☐ **Monograph** ☒ **Article thesis** ☐ **Essay thesis**

Abstract

Climate change, exacerbated by the increasing greenhouse gas emissions (GHG), has abruptly altered the life on Earth during the last few decades. Extreme weather, scarcity of fuels and natural resources, proliferating social inequalities and conflicts, are symptoms that the situation is getting out of hand. In this context, our energy systems, still dominated by the utilization of fossil fuels, are responsible for high emissions and air pollution, especially in cities. The decarbonization of heating and cooling networks is a priority, and ground-source heat pumps (GSHP) combined with underground thermal energy storage (UTES) offer an attractive technology to match supply and demand, allowing efficient integration of renewable energy sources and waste heat recycling.

This dissertation analyses in the first place the integration of GSHP and aquifer thermal energy storage (ATES) in both district heating and cooling networks, in terms of technoeconomic feasibility, efficiency, and impact on the aquifer. A holistic integration and a mathematical modeling of GSHP operation and energy system management are proposed and demonstrated throughout two case studies in Finland. Hydrogeological and geographic data from different Finnish data sources are retrieved for calibrating and validating the groundwater models, used to simulate the long-term impact of GSHP-ATES operation.

Another Finnish case study and large-scale GSHP / borehole thermal energy storage (BTES) application - Aalto New Campus Complex - is also investigated in this research. The specifically developed methodology for management of measured data is considered essential due to its capability to handle data with high uncertainty (thermal meters) by using highly accurate data regarding GSHP power demand. Operational data and relevant GSHP performance indicators are presented and analyzed, and a variety of measures for improving system operation are proposed. Additionally, several methods are developed for modeling the effective thermal resistance of groundwater-filled boreholes, deploying a working algorithm coupled with BTES simulation tool. It is observed that in real operation the effective thermal resistance can vary significantly, concluding that its update is crucial for a reliable long-term simulation of the BTES field.

The overall argument of this dissertation is that, even with limited and uncertain data, it is possible to assess the ATES integration for district heating and cooling with reasonable accuracy. By dispatching heating and cooling loads in a single operation, GSHP-ATES integration is technically viable and economically feasible, causing a limited long-term impact on the aquifer. Furthermore, the dissertation also highlights the importance of accurate monitoring and modeling of operating GSHP–BTES energy systems, including detailed modeling of their groundwater-filled boreholes - for efficient, reliable and sustainable long-term operation.

Keywords District Heating and Cooling, Geothermal Energy, Ground-Source Heat Pump (GSHP), Aquifer Thermal Energy Storage (ATES), Borehole Thermal Energy Storage (BTES), Mathematical and Groundwater Modeling, Optimization, Data Management

ISBN (printed) 978-952-64-0798-2 **ISBN (pdf)** 978-952-64-0799-9

ISSN (printed) 1799-4934 **ISSN (pdf)** 1799-4942

Location of publisher Helsinki **Location of printing** Helsinki **Year** 2022

Pages 168 **urn** http://urn.fi/URN:ISBN:978-952-64-0799-9

Aalto-yliopisto

Tiivistelmä

Aalto-yliopisto, PL 11000, 00076 Aalto www.aalto.fi

Tekijä
Oleg Todorov

Väitöskirjan nimi
Maalämpöpumput (GSHP) ja maanalainen lämpöenergiavarasto (UTES) – avainvektorit tulevaisuuden energiasiirtymään

Julkaisija Insinööritieteiden korkeakoulu

Yksikkö Konetekniikan laitos

Sarja Aalto University publication series DOCTORAL THESES 66/2022

Tutkimusala Energiatekniikka

Käsikirjoituksen pvm 15.02.2022 **Väitöspäivä** 27.05.2022

Väittelyluvan myöntämispäivä 28.04.2022 **Kieli** Englanti

☐ **Monografia** ☒ **Artikkeliväitöskirja** ☐ **Esseeväitöskirja**

Tiivistelmä

Ilmastonmuutos, jota pahentavat kasvavat kasvihuonekaasupäästöt, on muuttanut elämää maapallolla äkillisesti viime vuosikymmeninä. Äärimmäiset sääolosuhteet, polttoaineiden ja luonnonvarojen niukkuus, lisääntyvä sosiaalinen epätasa-arvo ja konfliktit ovat oireita siitä, että tilanne karkaa käsistä. Tässä yhteydessä energiajärjestelmämme, joita edelleen hallitsee fossiilisten polttoaineiden käyttö, ovat vastuussa korkeista päästöistä ja ilman saastumisesta erityisesti kaupungeissa. Rakennussektorin lämmitys- ja jäähdytysverkkojen dekarbonisaatio on etusijalla. Maalämpöpumput (GSHP) yhdistettyinä maanalaiseen lämpöenergian varastointiin tarjoavat kiinnostavan teknologian, joka vastaa kulutukseen ja tuotantoon mahdollistaen uusiutuvien energialähteiden tehokkaan integroinnin ja hukkalämmön kierrätyksen. Tutkimuksessa analysoidaan GSHP:n ja akviferi lämpöenergiavaraston (ATES) integrointia kaukolämpö- ja jäähdytysverkkoihin teknis-taloudellisen toteutettavuuden, tehokkuuden ja akviferin vaikutuksen kannalta. GSHP:n toiminnan ja energiajärjestelmän hallinnan kokonaisvaltaista integraatiota ja matemaattista mallintamista esitellään kahdessa suomalaisessa case-tutkimuksessa. GSHP-ATES:n toiminnan pitkäaikaisvaikutuksia simuloivien pohjavesimallien kalibroimiseksi ja validoimiseksi haetaan hydrogeologista ja maantieteellistä tietoa eri suomalaisista tietolähteistä.

Väitöskirjassa tutkitaan myös toista suomalaista case-tutkimusta ja laajamittaista GSHP/porauslämpöenergian varastointisovellusta (BTES) – Aalto-yliopiston uutta kampuskompleksia. Tähän erikseen kehitetty menetelmä mittaustietojen hallintaan on välttämätön, koska se pystyy käsittelemään dataa suurella epävarmuudella (lämpömittarit) käyttämällä tarkkaa dataa GSHP:n tehontarpeesta. Käyttötietoja ja relevantteja GSHP:n suoritusindikaattoreita analysoidaan ja ehdotetaan erilaisia toimenpiteitä järjestelmän toiminnan parantamiseksi. Lisäksi kehitetään useita menetelmiä pohjavedellä täytettyjen porausreikien tehollisen lämpöresistanssin arvioimiseen ja mallintamiseen käyttämällä työalgoritmia yhdistettynä BTES-simulaatiotyökaluun. On havaittu, että todellisessa käytössä tehollinen lämpöresistanssi voi vaihdella merkittävästi, ja siksi sen päivitys on ratkaisevaa BTES-kentän luotettavan pitkän aikavälin simuloinnin kannalta. Yleisenä argumenttina on, että rajallisella ja epävarmalla tiedolla on mahdollista arvioida ATES-integraatio kaukolämmön ja -jäähdytyksen osalta hyväksyttävällä tarkkuudella. Lähettämällä lämmitys- ja jäähdytyskuormat yhdellä kertaa, GSHP-ATES-integrointi on teknisesti kannattavaa ja taloudellisesti mahdollista. Silti sen vaikutus akviferiin on pitkäaikaisesti alhainen. Väitöskirja korostaa myös nykyisten GSHP–BTES-energiajärjestelmien tarkan seurannan ja mallintamisen tärkeyttä, mukaan lukien niiden pohjavedellä täytettyjen kaivojen yksityiskohtaisen mallintamisen tehokkaan, luotettavan ja kestävän pitkän aikavälin toiminnan kannalta.

Avainsanat Kaukolämpö ja -jäähdytys, geoterminen energia, maalämpöpumppu (GSHP), akviferi lämpöenergiavarasto (ATES), porareikälämpövarasto (BTES), matemaattinen ja pohjavesimallinnus, optimointi, tiedonhallinta

ISBN (painettu) 978-952-64-0798-2 **ISBN (pdf)** 978-952-64-0799-9

ISSN (painettu) 1799-4934 **ISSN (pdf)** 1799-4942

Julkaisupaikka Helsinki **Painopaikka** Helsinki **Vuosi** 2022

Sivumäärä 168 **urn** http://urn.fi/URN:ISBN:978-952-64-0799-9

Preface and Acknowledgements

"Traditionally, life has been divided into two main parts: a period of learning followed by a period of working. Very soon this traditional model will become utterly obsolete, and the only way for humans to stay in the game will be to keep learning throughout their lives, and to reinvent themselves repeatedly."
— Yuval Noah Harari, Homo Deus: A History of Tomorrow

"This is the essence of intuitive heuristics: when faced with a difficult question, we often answer an easier one instead, usually without noticing the substitution."
— Daniel Kahneman, Thinking, Fast and Slow

"Questions you cannot answer are usually far better for you than answers you cannot question."
— Yuval Noah Harari, 21 Lessons for the 21st Century

"Mediocracy encourages us in every possible way to doze rather than think, to view as inevitable what is unacceptable and as necessary what is revolting."
— Alain Deneault, Mediocracy

"It's when crisis hits - when the bombs fall or the floodwaters rise - that we humans become our best selves."
— Rutger Bregman, Humankind: A Hopeful History

We are living in a dynamic, dramatically changing, disruptive and convulsive world. It is immersed in a lethal and simultaneous combination of several ongoing crises - environmental, economic and societal - provoked by a suicidal necessity of continuous growth within the Planet with limited resources. During the past year, energy and food prices have skyrocketed to incredible levels exacerbated by the volatility of the markets, geopolitics and speculation. Natural disasters, extreme climate, scarcity of fuels and raw materials, increasing social inequalities and the recent Covid-19 pandemic only evidence how fragile we are.

In this context, our energy systems, unfortunately still highly dependent on fossil fuels, are generating carbon emissions and air pollution as well as jeopardizing the life on Earth. The reduction of carbon emissions and overall pollution is of vital importance, especially in cities. Furthermore, Europe's fossil fuel

energy dependence has been utilized as geopolitical intimidation weapon. Therefore, our priority is to get rid of coal, oil and gas as soon as possible. As part of the solution, ground source heat pumps (GSHP) in tandem with underground thermal energy storage (UTES) can play a crucial role for efficient and sustainable decarbonization of heating and cooling systems - in buildings and district energy networks.

The origins of the present research can be placed more than five years ago, starting with the work of Markku Virtanen related to aquifer thermal energy storage (ATES) application in Lahti, Finland. I had the privilege to work with Markku and learn from him that scientific work is fundamentally about leadership - based on mutual respect and cooperation - driven by personal example, moral authority and overall integrity. I am grateful to Prof. Markku Virtanen for this lesson, as I am to Dr. Kari Larjava and the team of Global EcoSolutions, Finland.

I wish to thank my supervising Prof. Risto Kosonen and Thesis Advisor Dr. Kari Alanne from Aalto University, my preliminary examiners Dr. José Acuña from KTH / Bengt Dahlgren, Sweden and Prof. Toke Rammer Nielsen from Technical University of Denmark, as well as my opponent Prof. Thomas Olofsson from Umeå University, Sweden. I wish to acknowledge also the collaboration with Dr. Antti Säynäjoki from Aalto University Campus & Real Estate.

I want to dedicate this work to my wife, Dr. Silja Siitonen - the Love of my life.

Helsinki, 20 April 2022
Oleg Todorov

Contents

List of Abbreviations

AF	Annuity Factor
AHU	Air Handling Unit
ANCC	Aalto New Campus Complex
ATES	Aquifer Thermal Energy Storage
BHE	Borehole Heat Exchanger
BTES	Borehole Thermal Energy Storage
CFF	Combined Frequency Factor
CP	Circulation Pump
COP	Coefficient of Performance
COP_{Car}	Carnot COP
COP_{Lor}	Lorentz COP
DC	District Cooling
DH	District Heating
DHW	Domestic Hot Water
DVR	Data Validation and Reconciliation
EED	Earth Energy Designer
EFT	Entering Fluid Temperature (GSHP evaporator)
FLS	Finite Line Source model
GDP	Gross Domestic Product
GHE	Ground Heat Exchanger
GHG	Greenhouse Gas
GRG	Generalized Reduced Gradient
GSHP	Ground Source Heat pump
GTK	Geological Survey of Finland
HP	Heat Pump
HVAC	Heat, Ventilation and Air Conditioning
LMTD	Logarithmic Mean Temperature Difference
NLSF	National Land Survey of Finland
ODA	Outdoor Dry Air Temperature
PF	Performance Factor
RES	Renewable Energy Sources
RMSE	Root Mean Squared Error
SPF	Seasonal Performance Factor
SEPEMO	Seasonal Performance factor and Monitoring for Heat Pump Systems
SYKE	Finnish Environment Institute
TRT	Thermal Response Test
UBW	Uniform Borehole Wall temperature
UHF	Uniform Heat Flux
VFD	Variable Frequency Drive
UTES	Underground Thermal Energy Storage

List of Publications

This doctoral dissertation consists of a summary and of the following publications which are referred to in the text by their numerals.

1. Todorov, Oleg; Alanne, Kari; Virtanen, Markku & Kosonen, Risto. (2020). A method and analysis of aquifer thermal energy storage (ATES) system for district heating and cooling: A case study in Finland. Sustainable Cities and Society, 53, 15 p. [101977]. https://doi.org/10.1016/j.scs.2019.101977.

2. Todorov, Oleg; Alanne, Kari; Virtanen, Markku & Kosonen, Risto. (2020). Aquifer Thermal Energy Storage (ATES) for District Heating and Cooling: A Novel Modeling Approach Applied in a Case Study of a Finnish Urban District. *Energies*, 13(10), 19 p. [2478]. https://doi.org/10.3390/en13102478.

3. Todorov, Oleg; Alanne, Kari; Virtanen, Markku & Kosonen, Risto. (2021). A Novel Data Management Methodology and Case Study for Monitoring and Performance Analysis of Large-Scale Ground Source Heat Pump (GSHP) and Borehole Thermal Energy Storage (BTES) System. *Energies*, 14(6), 25 p. [1523]. https://doi.org/10.3390/en14061523.

4. Todorov, Oleg; Alanne, Kari; Virtanen, Markku & Kosonen, Risto. (2021). Different approaches for evaluation and modeling of the effective thermal resistance of groundwater-filled boreholes. *Energies*, 14(21), 25 p. [6908]. https://doi.org/10.3390/en14216908

Author's Contribution

Publication 1: A method and analysis of aquifer thermal energy storage (ATES) system for district heating and cooling: A case study in Finland

The author of this dissertation carried out the investigation and conceptualization, developed the methodology, data analysis and validation as well as wrote the manuscript. Kari Alanne, Markku Virtanen and Risto Kosonen provided formal advising and supervision.

Publication 2: Aquifer Thermal Energy Storage (ATES) for District Heating and Cooling: A Novel Modeling Approach Applied in a Case Study of a Finnish Urban District

The author of this dissertation carried out the investigation and conceptualization, developed the methodology, data analysis and validation as well as wrote the manuscript. Kari Alanne, Markku Virtanen and Risto Kosonen provided formal advising and supervision.

Publication 3: A Novel Data Management Methodology and Case Study for Monitoring and Performance Analysis of Large-Scale Ground Source Heat Pump (GSHP) and Borehole Thermal Energy Storage (BTES) System

The author of this dissertation carried out the investigation and conceptualization, developed the methodology, data analysis and validation as well as wrote the manuscript. Kari Alanne, Markku Virtanen and Risto Kosonen provided formal advising and supervision.

Publication 4: Different approaches for evaluation and modeling of the effective thermal resistance of groundwater-filled boreholes

The author of this dissertation carried out the investigation and conceptualization, developed the methodology, data analysis and validation as well as wrote the manuscript. Kari Alanne, Markku Virtanen and Risto Kosonen provided formal advising and supervision.

1. Introduction

1.1 Background

Global warming, accelerated by the dangerous increase of greenhouse gas emissions (GHG), is one of the major concerns of the 21st century. In Europe, building sector accounts for 40% of the energy demand, while 80% of households' energy consumption correspond to heating, cooling and domestic hot water. The decarbonization of building sector is a priority European policy aiming to achieve an ambitious goal: 55% cut of GHG emissions by 2030 and zero-emission building stock by 2050, according to the recent proposal of the European Commission for Energy Performance of Buildings Directive (EPBD, 2021).

Worldwide, some 4.5 million people die prematurely every year due to air pollution generated by burning fossil fuels and the increased levels of PM2.5, while the overall cost is estimated as 3.3% of world gross domestic product (GDP) (Greenpeace, 2020). Over the next decade, environmental risks like "Climate action failure" and "Extreme weather" are top ranked in the 2022 World Economic Forum Global Risks Perception Survey (WEF, 2022), while threats like "Livelihood crisis" and "Social cohesion erosion" are the main societal concerns for the forthcoming five years. This situation is especially exacerbated in cities where nowadays live more than half of world population consuming over two-thirds of global energy demand. Therefore, a decarbonization of our existing energy networks, primarily based on fossil fuels generation, is a priority task for ensuring sustainable, healthy and socially fair future.

According to Eurostat (EU, 2018), in 2018 the share of renewable energy sources (RES) used for heating and cooling in the European Union was 21%. Several countries like Sweden (65%), Latvia (56%), Finland (55%) and Estonia (54%) covered more than half of their heating and cooling consumption with renewables sources (Eurostat 2020). The variability of renewable generation between heating and cooling seasons, as well as the low coincidence between supply and demand, are important challenges for RES penetration.

Shallow geothermal energy utilized in combination with heat pumps is considered essential for a future decarbonization of heating and cooling (IEA, 2021), particularly efficient when implemented in a centralized way and at district level (Hooimeijer and Maring, 2018). One of the most effective ways to reduce air pollution in cities and cut carbon emissions is by integrating ground source heat pumps (GSHP) within the existing heating and cooling networks (Paiho et al., 2018; Soltani et al., 2019; Popovski et al., 2019). The work of Paiho et al., 2018 revealed that large-scale heat pumps are crucial for increasing the

flexibility of the Finnish energy systems. Within the same research, different examples are presented for heat pump integration in Finnish district heating and cooling (DH/DC) networks: in Turku - the Kakola plant recycling heat from sewage wastewater, and in Helsinki - the Katri Vala plant generating heating and cooling in a single process.

The most utilized options for underground thermal energy storage (UTES) as a supplement to GSHPs, are aquifer thermal energy storage (ATES) as an open-loop solution, and borehole thermal energy storage (BTES) used in closed-loop. Wherever the hydrogeological conditions are favorable, ATES is an attractive technological option, suitable for large buildings and utilities (Fleuchaus et al., 2018) as well as capable to enable significant thermal storage capacities (Pellegrini et al., 2019). On the other hand, borehole thermal energy storage (BTES) and GSHPs systems are popular closed-loop solutions in the Nordic countries, where the existing geological conditions of hard bedrock and high groundwater levels (near the surface) determine the common utilization of vertical U-pipes within boreholes naturally filled with groundwater.

1.2 Aquifer Thermal Energy Storage (ATES)

The potential of ATES technology in tandem with GSHPs to be integrated as a sub-system of sustainable heating and cooling has been acknowledged worldwide. Short and long-term (seasonal) energy storage like ATES is needed for balancing supply and demand, efficient integration of renewable energy sources and waste heat as well as for increasing the overall system flexibility.

Bloemendal et al., (2015) developed a method for identifying the available world ATES potential combining climatic and hydro-geological data, as well as elaborated a world map for ATES suitability. The study concluded that some 50% of world urban areas have medium potential for ATES (remaining stable among the present century), while 15% have high potential - a figure which will decrease to 5% in the second half of the XXI century due to climate change. Lu et al., (2019) presented similar approach for evaluating world ATES potential based on socio-economic, geo-hydrological, climatic and groundwater factors, as well as concluded that ATES potential is very good, good and moderate in 7%, 20% and 34% of the zones respectively. Bayer et al., (2019) coined the concept of subsurface urban heat islands (SUHI) and concluded that large-scale urban subsurface temperature might be 2–6 °C higher than in the countryside. Consequently, cities, at least in Nordic conditions where heat extraction from ground is dominant, are the perfect candidates for GSHP-ATES integration.

Multiple investigations so far have been focused on ATES planning/monitoring in high density urban areas in terms of optimization of available subsurface space, flow/thermal interference and ATES overall efficiency (Bakr et al., 2013; Bloemendal et al., 2014; Bloemendal et al., 2018; Bozkaya et al., 2017; Caljé, 2010; Fleuchaus et al., 2020; Hoving et al., 2014; Sommer et al., 2015). Fleuchaus et al., 2018 presented a complete overview of global ATES development and application: some 3000 ATES systems are operated nowadays world-

wide, mostly located in Europe. The Netherlands with 85% of all ATES realizations followed by Sweden, Denmark and Belgium, are the undisputed frontrunners. From these 3000 ATES applications worldwide, there are some 100 large-scale utility systems, integrated in DH/DC networks (Schmidt et al., 2018).

ATES operation results in a combined hydrological, thermal, chemical and microbiological impact on the affected groundwater areas and should be carefully evaluated (Bonte et al., 2011). The legislation of shallow geothermal installations (depth less than 400 m) is diverse among countries (Haehnlein et al., 2010). Regulations for installations of wells concern the use of hazardous materials and proper backfilling of the drilling hole to avoid hydraulic short circuiting between aquifers. Other legislation concerns protection of groundwater areas for drinking water supply. Some countries adopt limits for minimum and maximum storage temperatures, like Austria (5–20 °C), Denmark (2–25 °C) and the Netherlands (5–25 °C) - while others adopt a maximum change in groundwater temperature, for example Switzerland (3 °C) and France (11 °C). That is why, a proper and accurate GSHP-ATES modeling is essential for assuring efficient and sustainable long-term ATES operation.

1.3 Borehole Thermal Energy Storage (BTES)

The energy footprint of buildings accounted for 29% of overall primary energy consumption globally in 2018, according to BP Energy Outlook 2020 (BP, 2020). In Europe, heating and cooling represent roughly half of all energy used in buildings and industry. As a result, making heating and cooling more sustainable and efficient is a priority for the European Commission (EC, 2016). In this context, ground source heat pumps (GSHP) in tandem with borehole thermal energy storage (BTES) is an attractive technological option for efficient dispatching of heating and cooling loads, the integration of renewable energy sources (RES), and waste heat. They are interesting also when aiming for further decarbonization of the existing heating and cooling networks (Connolly et al., 2014) and especially effective when applied in a centralized/shared way in a district level (Zhang et al., 2020).

The high potential of GSHP for efficient heating and cooling systems has fomented their exponential deployment and growth during the last decades. This has happened especially between 2015 and 2020 when their utilization almost doubled to 167 TWh/year and the installed capacity increased by 54%, reaching 77.5 GWt (Lund and Toth, 2021). Moreover, ground-coupled heat exchangers (GHE) and ground source heat pumps are commonly used in many medium and large-scale installations.

Finland is one of the top leading countries in heat pump utilization, with some 900,000 units, of which 140,000 are GSHP (Lund and Toth, 2021; Kallio, 2019). However, most of these heat pumps are small units installed in individual dwellings or apartment buildings, with still very few medium-/large-scale realizations. In 2019, Kallio estimated that there were only around 20–25 large-scale GSHP applications in Finland (applications with total borehole length over 10 km). One of these large-scale GSHP–BTES successfully operating projects in

Finland is the Aalto New Campus Complex (ANCC), with a total borehole length of 23 km powered by a GSHP with installed capacity of 800 kW_{th}. The GSHP is the heart of the energy system, providing simultaneously heating and cooling all year round. Therefore, accurate monitoring of the GSHP performance and its interaction with the BTES field is essential for efficient and sustainable operation in the long-term.

1.4 Long-term performance of large-scale GSHP

The increasing interest in evaluating the long-term performance of GSHP operation during the last decades has promoted different approaches such as the SEPEMO (Seasonal PErformance factor and MOnitoring for heat pump systems) schema (Nordman, 2012). SEPEMO defines four different system boundaries, e.g., the first boundary takes into account the heat pump (HP) refrigeration cycle, the second one additionally includes the power demand of the circulation pumps on the source-side, the third also considers the auxiliary heating and cooling, while the fourth additionally includes the distribution-side circulation pumps and fans (Spitler and Gehlin, 2019). The SEPEMO schema was primarily developed for noncomplex residential heat pump systems (not specifically GSHPs). Despite the significant effort done so far, there have been acknowledged certain limitations of SEPEMO boundary schema (HPT, 2020), especially when dealing with sophisticated GSHP configurations delivering simultaneously heating and cooling all year round (Spitler and Gehlin, 2019; Naicker and Rees, 2018).

1.5 IEA HPT Annex 52: performance analysis of complex GSHP

IEA HPT Annex 52 "Long-term performance measurement of GSHP systems for commercial, institutional and multi-family buildings" (Annex 52, 2021) is a 4-year-long (finalizing by the end of 2021) international project comprising 40 large-scale GSHP case studies from 7 participating countries (Gehlin and Spitler, 2021). IEA HPT Annex 52 has developed and enhanced the initial SEPEMO schema, including 6 boundaries (from 0 to 5) and additional indicator (a "+" superscript) for auxiliary heating/cooling. The proposed schema can be applied better for complex and large GSHP systems, however Spitler and Gehlin (2019) also acknowledged its limitations in some circumstances, like the complexity to allocate the power demand of the air handling units (AHU) separately to heating, cooling, and ventilation, which for example influences the correct implementation of system performance factors (PF) under boundary 4.

The author of this dissertation has been actively collaborating within the IEA HPT Annex 52 international working group, in the preparation and publication of the Finnish case study report (Todorov et al., 2021), which is mainly based on **Publications 3 and 4** of the present dissertation. Hopefully, the results from the annex would help building owners, designers and technicians evaluate, compare and optimize GSHP systems, and finally lead to energy and cost savings.

1.6 Effective thermal resistance of groundwater-filled boreholes

Borehole effective thermal resistance R_b* - in addition to ground thermal conductivity and undisturbed ground temperature - is one of the most important parameters to be determined during the initial thermal response tests (TRT) (Spitler and Gehlin, 2015). It is normally assumed that the initial estimation of borehole effective thermal resistance of groundwater-filled boreholes derived from TRT, is a fixed parameter. However, its value can vary significantly in real operation and depends on several factors like the regime of the fluid within the U-pipe (laminar/turbulent) and the natural convection of water within the borehole annulus (the space between the U-pipe and the borehole wall filled with groundwater). The natural convection, related to the buoyancy within the annulus apace, is mainly influenced by the heat rate (injection or extraction) and the annulus temperature (Javed and Spitler, 2016). Several studies have been focused on the experimental/modeling estimation of the effective thermal resistance of groundwater-filled boreholes subject to natural convection (Javed et al., 2012; Gustafsson and Westerlund, 2011; Spitler et al., 2016a).

Spitler et al. (2016a) derived experimental correlations for determining the convective heat transfer coefficients at the outer U-pipe surface and at the borehole wall as well as the effective thermal resistance of groundwater-filled boreholes. Their method is valid for little or no fractured bedrock (no groundwater advection) and relies on the calculation of the corresponding Rayleigh and Nusselt numbers in contact with borehole annulus, experimentally fitted to measured data of 5 TRT tests of groundwater-filled boreholes located in the Swedish Chalmers University of Technology. Johnsson and Adl-Zarrabi (2019) utilized Spitler's correlations and substituted the calculated values for groundwater-filled boreholes instead of those calculated for grouted boreholes, used within the GHE simulation toolbox *Pygfunction* (Cimmino et al., 2018). Johnsson et al. (2019) highlighted that the effect of natural convection in groundwater-filled boreholes was equivalent to grout material with 2–3 times better (higher) thermal conductivity than water.

1.7 Objective of the study

The main objective of the present research is to investigate the different possibilities for the application of ground source heat pumps (GSHP) in tandem with underground thermal energy storage (UTES). This objective finally aims at the gradual decarbonization of the existing heating and cooling networks, motivated by the increasing scarcity of fossil fuels and their devastating environmental impact on our Planet, acknowledged in the rapidly developing consequences of climate change.

In this respect, **Publications 1 and 2** focus on GSHP-ATES applications by investigating two case studies in Finland (located in Pukkila and Turku), while **publications 3 and 4** analyze different aspects of the operation of large GSHP-BTES system within the case study of the newly opened premises at Aalto University campus (Otaniemi, Espoo).

1.8 Novelty and content of the research

The novelty of the present research is to develop a practical methodology with hands-on approach based on two different Finnish case studies related to GSHP-ATES implementation and integration for district heating and cooling, analysis of their technoeconomic feasibility and the long-term impact on the aquifer. Moreover, it is concluded that this prefeasibility assessment can be done with an acceptable accuracy using limited and uncertain data. Other important topics, related to currently operating large-scale GSHP-BTES system (Aalto New Campus Complex), are also part of this dissertation: system monitoring, measured data management and performance assessment of GSHP real operation as well as specific modeling of groundwater-filled boreholes, long-term simulation and validation of the BTES field.

Publications 1 and 2 emphasize the importance of GSHP in tandem with UTES for efficient and sustainable decarbonization of the existing district energy networks, nowadays primarily based on the utilization of fossil fuels. They also deepen on how GSHP-ATES integration can be done in practice and propose a hands-on methodology for techno-economic evaluation, modeling and analysis of the long-term impact. The content of the publications can be summarized within the following main directions: methodology for the utilization of available Finnish open data sources related to hydrogeological and geographic conditions; mathematical and groundwater modeling of GSHP-ATES operation; development of different case studies analyzed in terms of efficiency and techno-economic feasibility; simulation and analysis of the long-term impact of GSHP-ATES operation.

Publication 3 is developing and implementing a novel data management methodology to assess the performance of a complex GSHP-BTES system under the conditions of high uncertainty related to measured data by the introduction of specific method for data validation and reconciliation (DVR). The particularly developed data management is considered essential due to its capability to adjust for consistency measured data with high uncertainty (thermal meters) by using highly accurate data (GSHP power demand). The proposed methodology is used also in conjunction with reconstruction of missing relevant data before April / May 2020 by applying linear regression techniques. Operational data and relevant GSHP performance indicators for the 18-month period starting from July 2019, is presented and analyzed within the Aalto New Campus Complex case study.

Aalto New Campus Complex (ANCC) is a new educational center at Aalto University, located in Otaniemi (Espoo), Finland. Within over 40 000 m^2, it comprises two faculties, a shopping center, recreational areas and a metro station. ANCC is also a significant large-scale application of GSHP-BTES in Finland, comprising an irregular BTES field of 74 boreholes with overall length of roughly 23 kilometers and 4 million m^3 of energy storage (Figure 1).

Figure 1. Aalto University New Campus Complex within the existing Otaniemi Campus.

Commonly used software tools for GHE modeling (Christodoulides et al., 2020) normally account for the effective thermal resistance of grouted boreholes, most of the tools assuming this resistance as constant during the simulation. In this regard, **Publication 4** introduces several approaches for analysis and evaluation of the effective thermal resistance (R_b*), specifically developed for groundwater-filled boreholes. They are based on the one hand on the utilization of monitoring data from distributed temperature sensing (DTS), by analyzing measured vertical borehole profiles, and on the other hand, with direct implementation of the recently developed correlations for groundwater-filled boreholes (Spitler et al., 2016a). The latter approach is deployed in a working algorithm, coupled with the python-based toolbox for GHE simulation *Pygfunction* and used to validate the initial 39 months of system operation.

Table 1. A topical framework of the research.

Studied topics	GSHP-ATES system		GSHP-BTES system	
	Publication 1	Publication 2	Publication 3	Publication 4
GSHP-UTES system integration for heating and cooling	✓ ATES reversible operation	✓ ATES one-way operation	✓ Irregular BTES field	✓ Irregular BTES field
Techno-economic feasibility	✓	✓		
Mathematical and groundwater modeling	✓	✓		
Long-term performance analysis and impact of system operation	✓ ATES hydraulic + thermal impact	✓ ATES hydraulic impact	✓ GSHP performance indicators	✓ BTES field simulation
Measured data management for consistency, data validation and reconciliation (DVR)			✓ Thermal energy meters	
Optimization used for DVR data management and borehole DTS thermal analysis			✓ DVR data management	✓ DTS thermal analysis
Borehole thermal analysis, modeling and validation				✓

1.9 Research questions

The main topic of the present dissertation is subdivided into seven research questions, summarized in Table 2. The first, second and third questions are related to GSHP-ATES systems and their integration, efficiency, techno-economic feasibility and long-term impact. Questions 4 and 5 deal with monitoring, data management and performance indicators of a large GSHP-BTES system, while the remaining questions 6 and 7 approach more specifically the modeling of groundwater-filled boreholes and its importance for long-term simulation of the BTES field.

RQ1: Is it possible to adequately integrate GSHP-ATES within the existing district heating and cooling networks?

RQ2: How can be assessed the energy system's efficiency and techno-economic feasibility?

RQ3: What is the GSHP-ATES long-term impact on the aquifer?

These research questions are addressed in **Publications 1 and 2** by proposing a hands-on methodology for GSHP-ATES integration and evaluation depending on different conditions like existing heating and cooling demand, hydro-geological conditions and other technical constraints as well as economic parameters and energy cost. Additionally, a methodology for the utilization of available Finnish open data sources related to hydrogeological and geographic conditions, is proposed for modeling and simulation of the long-term impact on the aquifer.

Table 2. Research questions and scope of the publications.

Research questions		GSHP-ATES system		GSHP-BTES system	
		Publication 1	Publication 2	Publication 3	Publication 4
RQ1	Is it possible to adequately integrate GSHP-ATES within the existing district heating and cooling networks?	✓	✓		
RQ2	How can be assessed the energy system's efficiency and techno-economic feasibility?	✓	✓		
RQ3	What is the GSHP-ATES long-term impact on the aquifer?	✓	✓		
RQ4	What are the challenges in retrieving and managing data from a complex GSHP-BTES system?			✓	
RQ5	How can relevant indicators be utilized for analyzing and improving the long-term system performance?			✓	
RQ6	How the effective thermal resistance of groundwater-filled boreholes can be evaluated in real operation?				✓
RQ7	Why appropriate modeling of groundwater-filled boreholes is crucial for a reliable long-term simulation?				✓

RQ4: What are the challenges in retrieving and managing data from a complex GSHP-BTES system?

RQ5: How can relevant indicators be utilized for analyzing and improving the long-term system performance?

These research questions are addressed in **Publication 3** by the implementation of specifically developed DVR methodology for management of measured data, highlighting the importance of long-term monitoring of system operation and performance analysis.

RQ6: How the effective thermal resistance of groundwater-filled boreholes can be evaluated in real operation?

RQ7: Why appropriate modeling of groundwater-filled boreholes is crucial for a reliable long-term simulation?

These research questions are addressed in **Publication 4** by the introduction of several methods for evaluation and modeling of the effective thermal resistance, specifically developed for groundwater-filled boreholes, and their application for reliable long-term simulation of the BTES field.

1.10 Structure of the dissertation

The dissertation comprises the summary of the published journal articles. The introduction (Section 1) presented the overall background of the study, its motivation and questions as well as how they are addressed within the publications. The following Section 2 introduces the methodology of the research while Section 3 highlights the fundamental results of the study. They are followed by discussion section (Section 4) and overall conclusions of the research (Section 5).

2. Methods

The research methods covered the design, implementation, techno-economic feasibility and long-term simulation of GSHP-ATES systems for district heating and cooling: **Publication 1** is developing a case study with reversible ATES operation, while **Publication 2** is introducing a case study with one-way ATES operation and two different scenarios.

On the other hand, **Publications 3 and 4** are dealing with complex GSHP-BTES systems, which methods are focused on the challenges in retrieving and managing of measured data for analyzing and improving system performance (**Publication 3**), while **Publication 4** is specifically focused on studying the effective borehole thermal resistance in real operation and how it can affect the long-term modeling of the BTES field.

2.1 GSHP-ATES systems for district heating and cooling

The modeling procedure of **Publications 1 and 2**, depicted in Figure 2, is based on the following steps, namely - i) input data of the target DH / DC networks and the nearby groundwater areas, ii) holistic integration (**Publication 1**) and mathematical modeling of combined ATES-GSHP operation (**Publication 2**), iii) techno-economic and sensitivity analysis, and iv) impact of ATES operation on aquifer areas, by developing and calibrating a specific groundwater model based on the finite difference method code MODFLOW (Harbaugh et al., 2005).

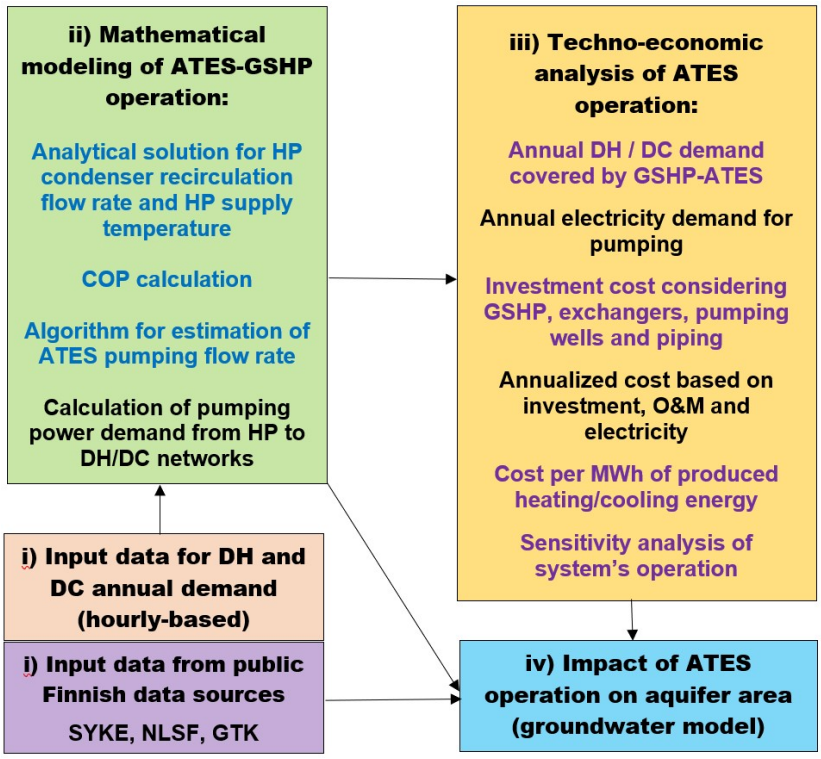

Figure 2. General modeling procedure of ATES-GSHP system for district heating and cooling.

2.1.1 Input Data of the DH and DC Networks

The target district heating and cooling networks are located in the central district of Kupittaa in the town of Turku (**Publication 2**), located in the southwest part of Finland and the available data of heating/cooling networks (heating/cooling demand and supply/return temperatures) is hourly based.

In **Publication 1**, an hourly-based simulation results for annual heating and cooling demand of office building (Tuominen et al., 2014) are used in order to introduce a dynamic variable cooling load, in addition to the real heating demand of Pukkila DH network. Operational temperatures were not available, thus assuming fixed DH supply temperature (80°C in winter and 70°C in summer with linear transition in fall/spring) and constant 40°C return temperature, as well as constant DC supply/return temperatures 10°C/16°C respectively.

The most relevant parameters of both case studies regarding their DH and DC networks are summarized in Table 3.

Table 3. Relevant parameters of DH / DC networks.

Relevant parameters of DH / DC networks	Publication 1 (Pukkila case study)		Publication 2 (Turku case study)	
	DH	DC	DH	DC
Annual energy demand, MWh	7,749	1,840	67,971	12,382
Maximum / minimum load, MW	3.26 / 0.26	2.56 / 0	27.06 / 0.43	6.38 / 0.52
Average load (± stand. dev.), MW	0.88 ± 0.6	0.21 ±0.4	7.76 ± 4.8	1.41 ± 0.7
Maximum / minimum supply temperature, ºC	80 / 70	10 / 10	110.4 / 56	10.0 / 5.3
Average supply temperature (± stand. dev.), ºC	74.2	10	84.3 ± 7.8	6.6 ± 0.3
Maximum / minimum return temperature, ºC	40 / 40	16 / 16	51.4 / 22.7	14.8 / 10
Average return temperature (± stand. dev.), ºC	40	16	40.9 ± 2.8	13.5 ± 0.4

2.1.2 Input Data of the Groundwater Areas

Data from the Finnish Environment Institute (SYKE, 2020) is used relative to groundwater areas, monitoring stations and observation wells. Pukkila aquifer (**Publication 1**) is composed of three different groundwater areas, of which two (#161602 and #161601) are close to Pukkila village and its district heating plant (located close to wells #605 and #705 used for ATES). Porvoonjoki River is a natural border of the south-eastern part of the village and separates area 161601 in two parts, being also a specified head boundary of the studied area (Figure 3).

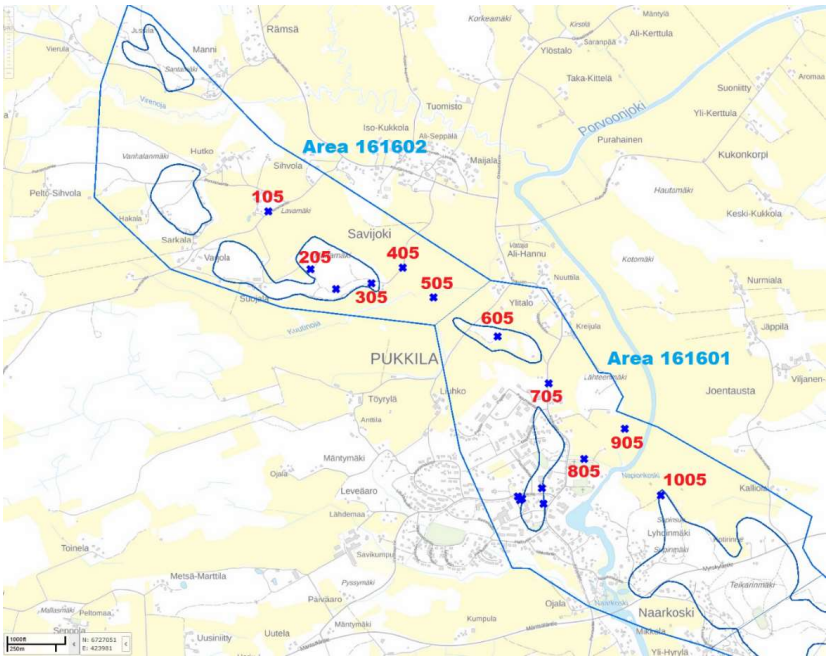

Figure 3. Pukkila groundwater areas and observation wells.

In **Publication 2** related to Turku case study, available information is utilized for 15 observation wells located in HK-Ruokatalo area (near-field) of Kupittaa district and 8 wells in Kaarninko area (far-field), and their long-term statistical data for average head are used for steady state model calibration, as shown in Figure 4.

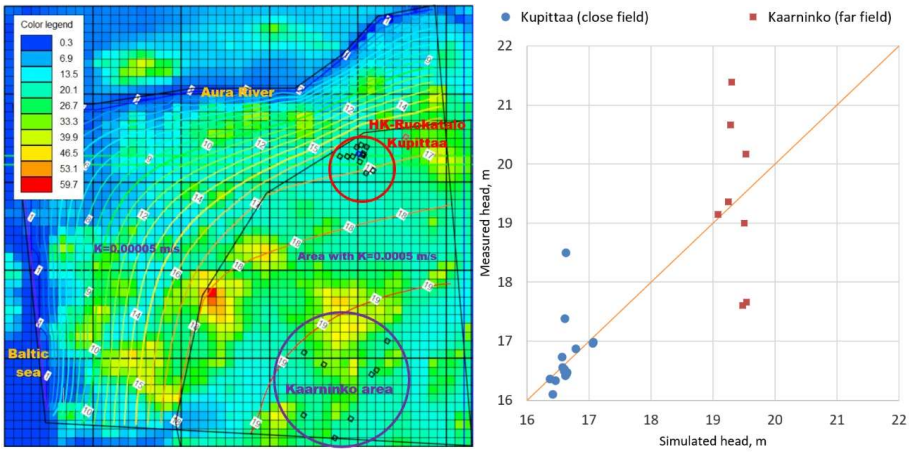

(a) **(b)**

Figure 4. Kupittaa (Turku) groundwater areas, observation wells and steady state model calibration (a) and measured vs. simulated head comparison for steady state (b).

The main properties of the studied groundwater areas and their observation wells are summarized in Table 4.

Table 4. Groundwater areas (observation wells).

Groundwater areas	Publication 1 (Pukkila case study)	Publication 2 (Turku case study)
Number of near-field observation wells	4 (excluded #1005)	15
Number of far-field observation wells	5	8
Average head near-field wells, [m a.s.l.]	44.80	16.74
Average head far-field wells, [m a.s.l.]	49.22	19.37
Average undisturbed aquifer temperature, [°C]	7	10

2.1.3 Geographical Data

In both **Publications 1 and 2**, open data from the National Land Survey of Finland (NLSF, 2020) is used, particularly its "10m elevation model". The elevation model was retrieved as Geo-TIFF raster file and transformed to Surfer Grid file (GRD) using QGIS software (QGIS, 2020). For example, in Figure 4 (a) the color legend represents terrain elevations in meters above sea level (a.s.l.).

2.1.4 ATES-GSHP integration for district heating and cooling

Ground-source heat pump, operating with abstraction and injection well (well doublet) is considered in both case studies. The condenser side of the heat pump is connected to the DH network while the evaporator side is connected to aquifer pumping stream.

In **Publication 1**, a 0.35 MW_{th} capacity GSHP is used to fulfil partially the heating demand (heat pump used as base load, covering domestic hot water (DHW) in summer), using the existing chips boiler for peak loads. If boiler is needed, GSHP would be used first to increase DH network temperature from 40°C (assumed return temperature) to some intermediate value, and after that, the final DH supply temperature would be reached by the boiler. Different and reversible operation during summer and winter periods is assumed, creating an ATES well doublet - warm well (#605, Figure 3) and cold well (#705). During the summer operation a primary ATES circuit starts from the cold abstraction well, providing district cooling. After the cooling exchanger, water at up to 14°C is utilized in GSHP evaporator, and finally injected into the warm well. During the winter period the process is reversed; water is taken from the warm well, conducted if needed through the district cooling network exchanger, used with GSHP, and finally injected into the cold well (see Figure 5). The average aquifer abstraction temperatures from the warm and cold wells are estimated iteratively as 7.3°C and 3.9°C respectively (see **Publication 1** for more details).

While **Publication 1** presented a GSHP-ATES integration centrally in a heat plant (before the peak load boiler), **Publication 2**, on the other hand, introduced a GSHP integration as a part of DH/DC branch of urban district, utilizing one-way ATES operation. Within the first scenario (GSHP capacity 1.4 MW_{th}), the ATES pumping flow path encounters two serial exchangers – HP evaporator and cooling for DC network. In the second scenario, with GSHP capacity 1.6 MW_{th}, before the HP evaporator, a pre-cooling exchanger is added, providing a first stage cooling to the DC network. With this configuration the DC demand can be more efficiently covered and GSHP efficiency (COP) is improved since heat pump inlet temperature increases several degrees after a pre-cooling exchanger. ATES-GSHP integration within the existing DH/DC networks is depicted in the general scheme presented in Figure 6, where temperature values illustrate the second scenario setup. The average aquifer abstraction temperature is assumed equal to aquifer undisturbed temperature (10°C).

In **Publication** 2, GSHP is utilized to recover and upgrade all excess heat proceeding from the DC network and inject it into DH network. In this sense, ATES is utilized for balancing the energy system and mitigating the variability and no-coincidence of the simultaneously dispatched heating and cooling loads. For this purpose, heat pump supply temperature is calculated, based on the demanded power fraction k (the ratio between heat supplied by the heat pump and total heat demanded in the DH branch). The flow fraction recirculated through HP condenser can be calculated as: k^p, where $0 \leq p \leq 1$ is additional exponent parameter (chosen equal to 0.6), thus the ratio between heat pump condenser temperature difference ΔT_{HPC} and overall temperature difference ΔT_{DH} of DH

network is $k^{1\text{-}p}$ (Figure 6). With this arrangement HP supply temperature is lower than DH supply, which in turn improves the heat pump COP.

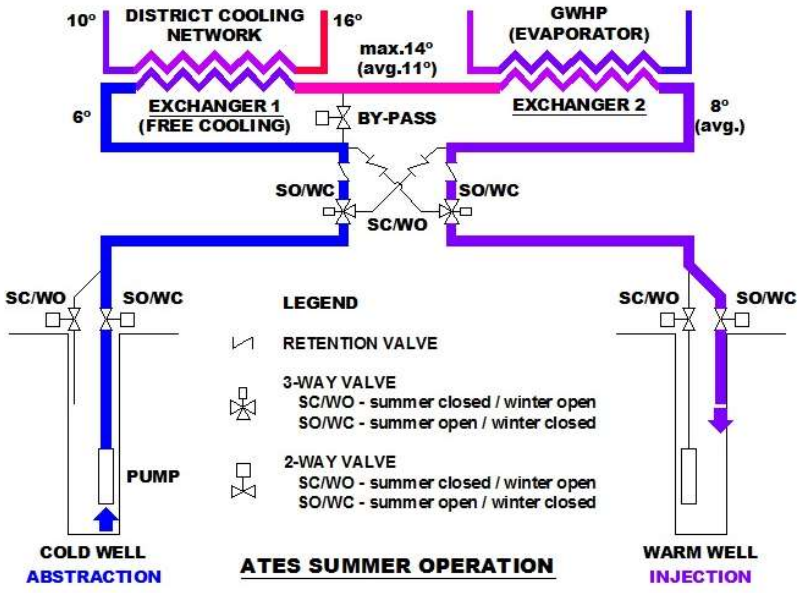

(a)

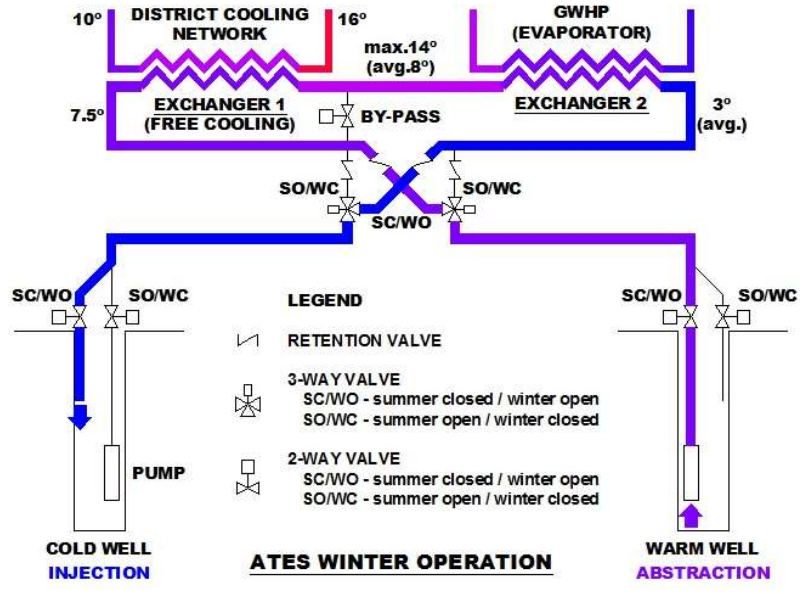

(b)

Figure 5. Reversible ATES operation (Publication 1) in summer mode (a) and winter mode (b).

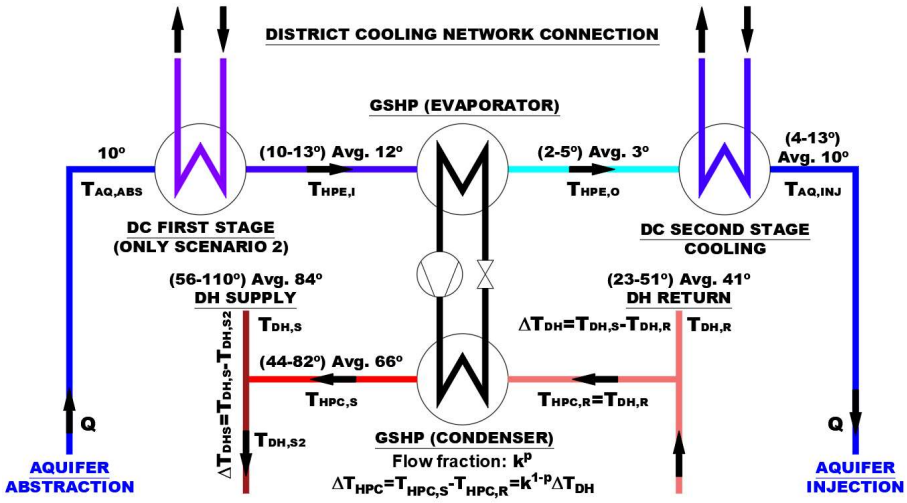

Figure 6. One-way ATES operation (Publication 2, temperature values refer to Scenario 2).

2.1.5 Estimation model of heat pump COP

In **Publication 1**, a simplified linear regression model based on GSHP producer's data (Pero, 2016) is implemented. Available data is used for four source temperatures T_1 (0°, 10°, 20° and 30°) and five HP supply temperatures T_2 (40°, 50°, 60°, 70° and 80°), estimating HP COP as follows:

$$\mathrm{COP} = a \cdot T_2 + b \quad (1)$$

while parameters a and b depend on source temperatures T_1 according to the following relation (Table 5):

Table 5. COP parameters *a* and *b* vs. evaporator source temperature T_1.

Source temperature T_1, °C	0	10	20	30
Parameter *a*	-0.045	-0.061	-0.08	-0.103
Parameter *b*	5.5	7.06	9	11.3

On the other hand, **Publication 2** utilized Lorentz COP, defined as follows (Reinholdt et al., 2018):

$$COP = \frac{\eta T_{lm,H}}{T_{lm,H} - T_{lm,L}} \quad (2)$$

$$where\ T_{lm,H} = \frac{T_{HPC,S} - T_{HPC,R}}{ln\left(\frac{T_{HPC,S}}{T_{HPC,R}}\right)};\ T_{lm,L} = \frac{T_{HPE,O} - T_{HPE,I}}{ln\left(\frac{T_{HPE,O}}{T_{HPE,I}}\right)}$$

$T_{lm,H}$ and $T_{lm,L}$ are respectively the logarithmic mean temperature of the sink and source, where index notations *HPC* and *HPE* stand for heat pump´s condenser and evaporator temperatures, while notations *I* / *O* stand for inlet / out-

let temperatures of the evaporator and S / R stand for supply / return temperatures of the condenser (all values expressed in Kelvin). Based on best industrial refrigeration systems, Reinholdt (2018) suggested values for Lorentz efficiency η between 50 and 60%. In Kupittaa (Turku) case study, a more conservative value of 45% is adopted.

2.1.6 Computation of ATES pumping flow rate

For each timestep n of system operation, it is challenging to determine the needed (as low as possible) ATES pumping flow rate Q_n, since there is a constraint for daily pumping of the specific groundwater area (i.e., in **Publication 2** it is 2500 m³/day). In **Publication 1**, the ATES pumping flow rate is calculated on a daily basis as a maximum value between the flow needed for heating and the flow needed for cooling (heat pump COP estimated with Equation (1)).

In **Publication 2**, the ATES pumping flow is estimated iteratively. If $\Phi_{heat,n}$ and $\Phi_{cool,n}$ are respectively the heating and cooling demand to be covered in hour n, the pumping flow can be estimated as the maximum flow needed either for heating or cooling (iterative estimation for Q_n):

$$Q_n: max\left\{\frac{\left(1-\frac{1}{COP_n}\right)\emptyset_{heat,n}}{S_{VC,wat}\left(T_{HPE,I,n}-T_{HPE,O,n}\right)}; \frac{\emptyset_{cool,n}}{S_{VC,wat}\left(T_{HPE,I,n}-T_{AQ,ABS,n}+T_{AQ,INJ,n}-T_{HPE,O,n}\right)}\right\} \quad (3)$$

$$T_{HPE,I,n} = T_{AQ,ABS,n}\ (in\ sc.1)\ ;\ T_{HPE,I,n} = max\{T_{AQ,ABS,n}; T_{DC,R,n} - \Delta T_{min}\}\ (sc.2)$$

$$T_{AQ,INJ,n,max} = T_{DC,R,n} - \Delta T_{min}\ ; T_{HPE,O,n,min} = 2°C;\ S_{VC,wat} = 4.19\ MJ/m^3K$$

Where $T_{AQ,ABS,n}$ / $T_{AQ,INJ,n}$ are respectively aquifer abstraction/ injection temperatures, $T_{DC,R,n}$ is district cooling return temperature, ΔT_{min} = 2 °C is the minimum pinch point difference in cooling exchangers and $T_{HPE,O,n,min}$ = 2 °C is the minimum temperature after GSHP evaporator. COP_n is calculated with Equation (2), assuming average values for evaporator inlet temperature $T_{HPE,I}$ = 10 °C (12 °C for Scenario 2), and evaporator outlet temperature $T_{HPE,O}$ = 2 °C (3 °C for Scenario 2). An illustration of ATES flow path (Scenario 2) with all temperature constraints is shown in Fig. 7.

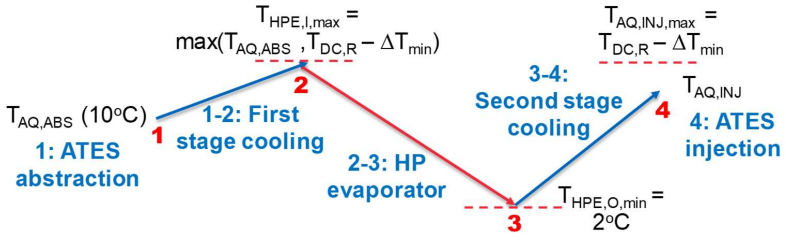

Figure 7. ATES flow path in Scenario 2 (Publication 2).

The iteration for Q_n depends on the studied scenario (Scenario 1 – no precooling exchanger / Scenario 2 – first stage DC exchanger):

Scenario 1: Recalculation of temperature after HP evaporator (for hour n)

$$T_{HPE,O,n} = T_{HPE,I,n} - \frac{\left(1 - \frac{1}{COP_n}\right) \emptyset_{heat,n}}{S_{VC,wat} \cdot Q_n} \quad (4)$$

Scenario 2: Recalculation of 1st and 2nd stage cooling loads covered

$$\emptyset_{cool-1stag\ ,n} = Q_n S_{VC,wat}\left(T_{HPE,I,n} - T_{AQ,ABS,n}\right)$$

$$T_{HPE,O,n} = T_{HPE,I,n} - \frac{\left(1 - \frac{1}{COP_n}\right) \emptyset_{heat,n}}{S_{VC,wat} \cdot Q_n} \quad (5)$$

$$\emptyset_{cool-2stage,n} = min\left\{Q_n S_{VC,wat}\left(T_{AQ,INJ,n} - T_{HPE,O,n}\right); \emptyset_{cool,n} - \emptyset_{cool-1stage,n}\right\}$$

$$\emptyset_{cool,n} = \emptyset_{cool-1stag\ ,n} + \emptyset_{cool-2stage,n}$$

The ATES flow Q_n is recalculated again with Equation (3), until the new value deviates from the previous less than a predefined threshold (±5%).

2.1.7 Calculation of ATES pumping power demand

The required pumping power [kW] for ATES operation is calculated, based on ATES flow rate Q_n, assuming overall pressure drop in the line Δp = 600 kPa and standard pumping efficiency η = 0.55 (Grundfos, 2020a):

$$P_{ATES,n} = \frac{Q_n \Delta p}{\eta} \quad (6)$$

2.1.8 Calculation of pumping power demand to DH/DC network

In **Publication 2**, the pumping power [kW] to provide DH/DC through GSHP condenser / evaporator respectively is calculated based on the condenser / evaporator flow rates $Q_{HPC,n}$ / $Q_{HPC,n}$, assuming overall pressure drop between supply and return lines $\Delta p_{DH} = \Delta p_{DC}$ = 250 kPa (EUROHEAT, 2008) and standard pumping efficiency η = 0.55 (Grundfos, 2020b):

$$P_{HPC-to-DH,n} = \frac{Q_{HPC,n} \Delta p_{DH}}{\eta} \; ; \; P_{HPE-to-D\ ,n} = \frac{Q_{HPE,n} \Delta p_{DC}}{\eta} \quad (7)$$

$$Q_{HPC,n} = \frac{\emptyset_{supplied-heat,n}}{S_{VC,wat}\left(T_{HPC,S,n} - T_{DH,R,n}\right)} \; ; \; Q_{HPE,n} = \frac{\emptyset_{cool-1stage,n} + \emptyset_{cool-2stag\ ,n}}{S_{VC,wat}\left(T_{DC,R,n} - T_{DC,S,n}\right)}$$

The volumetric heat capacity of water $S_{VC,wat}$ used is 4.19 and 4.1 MJ/m³K respectively for cooling and heating operation.

2.1.9 Techno-economic evaluation of GSHP-ATES operation

In both case studies, different technical variables are computed, like the annual energy generation for heating and cooling, the electricity consumption of both GSHP and pumping as well as the average daily ATES pumping rate. Table 6 lists the relevant ATES technical variables.

Table 6. Technical variables of ATES-GSHP operation.

Variables	Units	Comments
GSHP supply temperature	ºC	Depending on demanded heat power fraction (*k*)
GSHP COP	-	Depending on GSHP source and sink temperatures
ATES flow rate *Q*	m^3/s	In Publication 1: Estimated as the maximum flow rate needed either for heating or cooling In Publication 2: Calculated iteratively
GSHP electric power demand	MW	Based on HP heat load covered and COP
Electric power demand for ATES pumping	kW	Based on the computed flow rate Q, assumed pressure drop and pumping efficiency
Electric power demand for DH / DC pumping	kW	Based on the computed flow rate for each network, assumed pressure drop and pumping efficiency (only in Publication 2)
Daily ATES flow rate	m^3/day	Average daily ATES flow rate
Annual heating demand	MWh	Heating demand covered by GSHP
Annual cooling demand	MWh	Cooling demand covered by ATES-GSHP
Annual GSHP demand	MWh	Electricity demand of GSHP
Annual pumping demand	MWh	Pumping demand of ATES. DH and DC pumping is considered only in Publication 2

Cost database regarding various energy generation technologies is used (Nielsen et al., 2013 and DEA. 2020), as well as prices for ATES well drilling, heat exchangers and piping (Drenkelfort et al., 2014) for estimating the investment cost. Based on the annuity factor (AF) method (**Publications 1 and 2**), the energy generation cost is calculated, assigning annual investment payments (annuity) and assuming 5% interest rate as well as investment's lifetime of 20 years (Nielsen et al., 2013). O&M costs (1% of investment) are also included within the overall annual cost, as well as the electricity cost for GSHP and pumping (given electricity price of 100 €/MWh, including taxes, transfer and distribution fees, according to NORDPOOL. 2020). The economic evaluation is developed including the calculation of the following variables listed in Table 7.

Table 7. Variables for economic evaluation.

Variables	Units	Comments
Overall investment cost	€	Geological survey, GSHP, exchangers, drilling and piping
Annuity factor	-	Computed for 20 years lifetime and 5% interest rate
Investment cost (annuity)	€	Calculated as overall investment cost times annuity factor
Fixed annual O&M costs	€	1% of overall investment cost
Electricity annual cost	€	Electricity cost of GSHP and pumping
Overall annual cost	€	Annuity + O&M costs + electricity cost
Specific energy cost	€/MWh	Overall annual cost per total thermal energy generation

2.1.10 Groundwater model and long-term ATES operation

The groundwater model is set up utilizing the finite difference model (FDM) MODFLOW (Harbaugh et al., 2005) with ModelMuse environment (ModelMuse, 2022). In **Publication 2**, the aquifer is discretized with a 100x100 m square cell grid, covering a physical extension of about 20 km^2, delimited between the Aura River to the northwest and the Baltic Sea to the southwest. Southeast and northeast borders are no-flow boundaries (see Figure 4).

Similarly, In **Publication 1**, the aquifer area is discretized using 100x100m square cell and grid of 40 columns by 13 rows, covering a physical area of roughly 3 km^2, comprised between the aquifer north-west border and the natu-

ral boundary, Porvoonjoki River, from the east (Figure 3). Additionally, the solute transport model MT3DMS (Zheng et al., 1999) is used to simulate the heat transport in shallow confined aquifers due to similarities between the mathematical formulation of solute and heat transport equations (Hecht-Méndez et al., 2010a/2010b). Local grid refinement (LGR) is adopted in the MODFLOW/MT3DMS model, where nearby areas to warm and cold wells are discretized with 50x50m cell size. The most relevant parameters of the groundwater models used in both publications are shown in Table 8.

Table 8. Groundwater models (relevant parameters).

Groundwater models for long-term simulation (relevant parameters)	Publication 1 (Pukkila case study)	Publication 2 (Turku case study)
FDM modeling tools	MODFLOW / MT3DMS	MODFLOW
Discretization grid	100x100m / LGR 50x50m near the pumping wells	100x100m
Model extension, km^2	3	20
Long-term simulation, years	20	20
Specified head boundaries	Porvoonjoki River, Virenoja / Kuutinoja Streams	Aura River, Baltic Sea
Aquifer type and thickness	Confined, 20m	Confined, 10m
Undisturbed aquifer temperature, ºC	7	10
Aquifer hydraulic conductivity K, m/s	$1x10^{-3}$	$5x10^{-5}$ / $5x10^{-4}$
Aquifer storativity S	$1x10^{-5}$	$1x10^{-5}$
Aquifer recharge R, m/s	$6x10^{-9}$	$1.3x10^{-8}$
Aquifer porosity	0.25	0.25
Distribution coefficient K_d (MT3DMS), m^3/kg	$2.1x10^{-4}$	-
Diffusion coefficient D_m (MT3DMS), m^2/s	$1.9x10^{-6}$	-
Longitudinal dispersivity α (MT3DMS), m	0.5	-

2.2 Performance analysis of large-scale GSHP-BTES system

Publications 3 and 4 are dealing with the new academic center of Aalto University, a large-scale application of Ground Source Heat Pump (GSHP)–Borehole Thermal Energy Storage (BTES) in Finland.

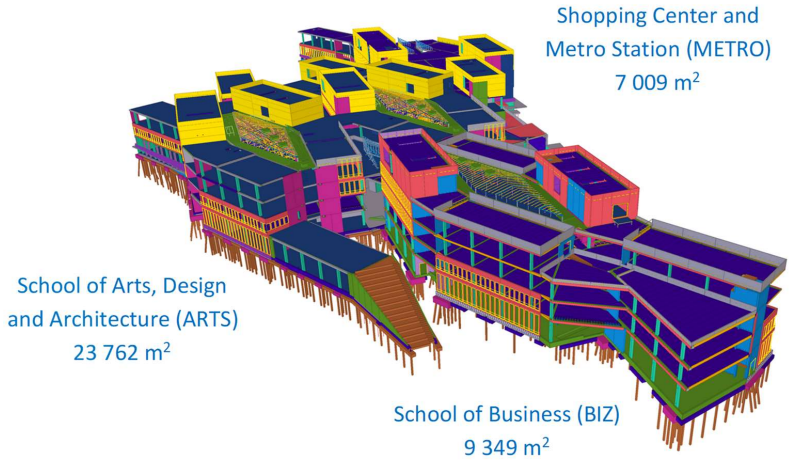

Figure 8. General schematics of Aalto New Campus Complex (courtesy of Tekla, Finland).

Aalto New Campus Complex (ANCC) located in Otaniemi (Espoo), is a 40,000 m² polyfunctional 4/5-storey modern building (Figure 8) and includes the following main parts: the School of Arts, Design, and Architecture (ARTS); the School of Business (BIZ); as well as a shopping center, recreational areas, cafeterias, restaurants, and a metro station (METRO).

The heart of the ANCC energy system is the GSHP, composed of nine centralized heat pump modules operating in a cascade mode, with a total nominal capacity of 0.8 MW_{th}. Heat pump modules generate simultaneously heating on the condenser side and cooling on the evaporator side, and are connected to an irregular BTES field composed of 74 300-m-deep groundwater-filled boreholes.

Additionally, the energy system is connected to a DH network, which is utilized as a peak heat source in addition to the GSHP. Domestic hot water (DHW) is directly generated by DH, thus the GSHP is used only for heating. Overall, heating is delivered within a low temperature network (supply temperature 30–45°C, compensated depending on outdoor temperature) through three different circuits: AHU-heating, space heating and snow melting (see Figure 9). The maximum return temperature is set to 30°C and every time it surpasses this value (in summer), excess heat is dissipated. On the other hand, space cooling is provided all year round through radiant systems (supply/return temperatures 12–16°C/15-18°C). AHU-cooling is operating only with high cooling demand (in summer mode, it is assisted by the heat pump), however it cannot utilize directly the BTES source. There is limited possibility for indirect AHU free-cooling through the space-cooling circuit, which in practice creates a free-cooling bottleneck. The switching between summer and winter operation depends on several parameters like the outdoor dry air temperature (ODA), cooling demand, temperatures of the cooling circuits, etc. It happens normally with ODA between 12°C and 15°C.

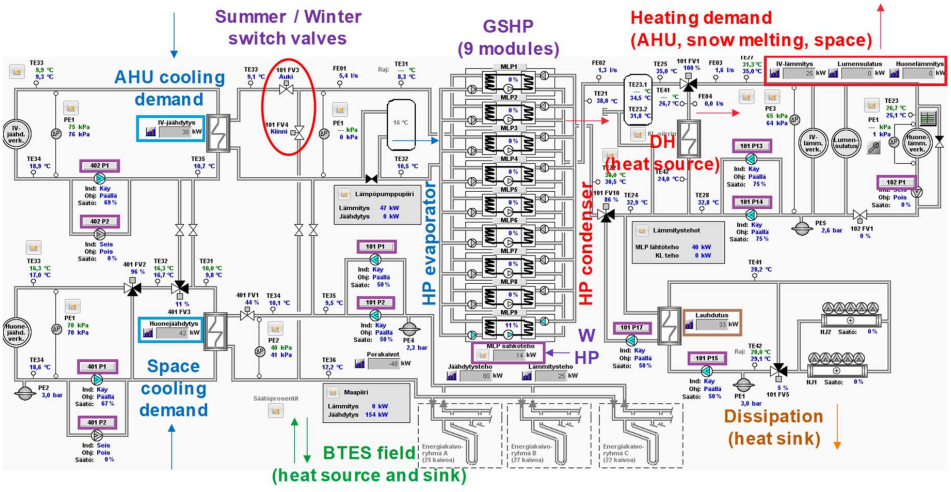

Figure 9. Energy system: HVAC and GSHP-BTES general scheme.

Within the monitoring system of ANCC, there are 12 thermal energy meters measuring heating and cooling demand (both AHU- and space- demand) of 3

different zones, namely: the School of Business (BIZ), the Metro station (METRO) and both Schools of Arts and Business (ARTS+BIZ). Additionally, there are 3 thermal energy meters for measuring the BTES field, snow melting and dissipation energy, respectively. The nomenclature of all thermal energy meters of ANCC is presented in Table 9.

Table 9. Nomenclature of thermal energy meters in ANCC.

Zone / Type	AHU-cooling	Space cooling	AHU-heating	Space heating	Others
ARTS+BIZ	402 LM01	401 LM01	101 LM03	102 LM01	-
METRO	402 LM02	401 LM02	101 LM04	102 LM02	-
BIZ	402 LM03	401 LM03	101 LM05	102 LM03	-
BTES field	-	-	-	-	101 LM01
Dissipation	-	-	-	-	101 LM02
Snow melting	-	-	-	-	191 LM01

The heating and cooling demands of the ANCC have been monitored since July 2019. However, loads of the BTES field and dissipation have been acquired only since April / May 2020. All thermal energy meters are not calibrated yet, and there is a high uncertainty regarding their measurements due to the following reasons:

- The accuracy of energy meters depends on different factors: errors related to the flow, delta T of sensors, calculator, quality of installation, proximity to disturbances and pumps, dirt in fluid, gas entrainment, sampling interval, etc. (Butler et al., 2016).
- ANCC meters record data only once per hour regarding flow, temperature and energy (instead of doing it more frequently, with reduced sampling interval). This can generate significant errors which are difficult to estimate without calibration.
- All ANCC meters are battery powered, thus the sampling interval can be an issue, since a much longer sample interval is used to reduce power consumption (Butler et al., 2016). Meters with slow response can cause significant errors around 20-30% (Butler et al., 2016).
- The location of most of the energy meters is far away (sometimes hundreds of meters of pipe connections) from the main HVAC room, thus heat losses / gains in distribution pipes and heat exchangers are not accounted for and can introduce additional errors.

2.2.1 A data management methodology to assess the performance of a complex GSHP-BTES system

A specifically developed data validation and reconciliation (DVR) procedure with daily resolution is adopted due to the significant thermal inertia of both heating and cooling hydraulic networks, which in practice makes impossible to achieve e.g., hourly-based balance on both sides of the GSHP. This resolution is good enough for depicting system daily operation, however it is not able to capture more precise energy ramping or hourly-based peak loads.

The proposed methodology is used in conjunction with a reconstruction of missing relevant data before April / May 2020 allowing a reconstruction of the whole energy system since July 2019. Therefore, the proposed methodology is

essential due to its capability to handle measured data with high uncertainty (thermal meters) by using highly accurate data (power meters) as a robust procedure balancing the evaporator and condenser side of the GSHP.

Four different uncertainty factors were introduced for all measured heating, cooling, BTES and dissipation loads respectively in order to accomplish a daily balance on both the evaporator and condenser side of the GSHP.

Relative errors $\Delta_{evap,i}$ and $\Delta_{cond,i}$ are formulated on both sides of GSHP for each day i of operation:

$$\Delta_{evap,i} = \frac{Q_{evap,i} + Q_{cool,i} f_{cool,i} + Q_{BTES,i} f_{BTES,i}}{Q_{evap,i}}$$
$$\Delta_{cond,i} = \frac{Q_{cond,i} + Q_{DH,i} - Q_{heat,i} f_{heat,i} - Q_{diss,i} f_{diss,i}}{Q_{cond,i}} \quad (8)$$

where $Q_{cool,i}$ and $Q_{heat,i}$ are respectively total measured cooling demand (negative sign) and total heating demand (positive sign) [MWh]

$Q_{evap,i}$ and $Q_{cond,i}$ are the GSHP loads on the evaporator / condenser side [MWh] (positive sign, they are not measured and are determined with the DVR procedure)

$Q_{DH,i}$, $Q_{BTES,i}$ and $Q_{diss,i}$ are the measured loads related to DH (net input for heating, positive sign), BTES (negative for heat extraction from the ground and positive for heat injection) and dissipation (positive sign), respectively [MWh]

$f_{cool,i}$, $f_{BTES,i}$, $f_{heat,i}$ and $f_{diss,i}$ are the uncertainty factors for cooling, BTES, heating and dissipation.

2.2.2 Optimization problem for data management

The optimization problem is defined in order to minimize the sum of squared relative errors $\Delta_{evap,i}$ and $\Delta_{cond,i}$ (eventually to 0) by varying the aforementioned uncertainty factors $f_{cool,i}$, $f_{BTES,i}$, $f_{heat,i}$, $f_{diss,i}$ and the loads on the condenser $Q_{cond,i}$. It operates with daily values and is formulated on a monthly basis (n is the number of days in a month):

Objective function:

$$min\ z = \sum_{i=1}^{n} \Delta_{evap,i}^2 + \sum_{i=1}^{n} \Delta_{cond,i}^2 \quad (9)$$

Subject to constraints:

$Q_{evap,i} = Q_{cond,i} - W_{HP,i}$, where $W_{HP,i}$ *is the GSHP power demand*

$Q_{cond,i}$, $Q_{evap,i}$, $f_{cool,i}$, $f_{BTES,i}$, $f_{heat,i}$, $f_{diss,i} \geq 0$ (non-negative condition)

The initial values of all uncertainty factors are set to 1, while the initial values of HP condenser $Q_{cond,i}$. are chosen in order to fulfil the balance on the condenser side ($\Delta_{cond,i} = 0$). The optimization problem is solved using the GRG nonlinear method in MS Excel Solver. The obtained uncertainty factors with the optimization procedure are used to adjust the loads by multiplying them with the corresponding uncertainty factors: total cooling demand $Q_{cool,I}$ composed of AHU-

cooling $Q_{AHU\text{-}cool,i}$ and space-cooling $Q_{spa\text{-}cool,i}$; BTES loads $Q_{BTES,i}$; total heating demand $Q_{heat,i}$ composed of AHU-heating $Q_{AHU\text{-}heat,i}$, space-heating $Q_{spa\text{-}heat,i}$ and snow melting $Q_{snow\text{-}melt,i}$; dissipation loads $Q_{diss,i}$. The adjusted data fulfil the necessary energy balances on both sides of the GSHP (evaporator and condenser, which loads are also determined) and therefore is consistent. The detailed procedure applied for data management in **Publication 3** is shown in Figure 10.

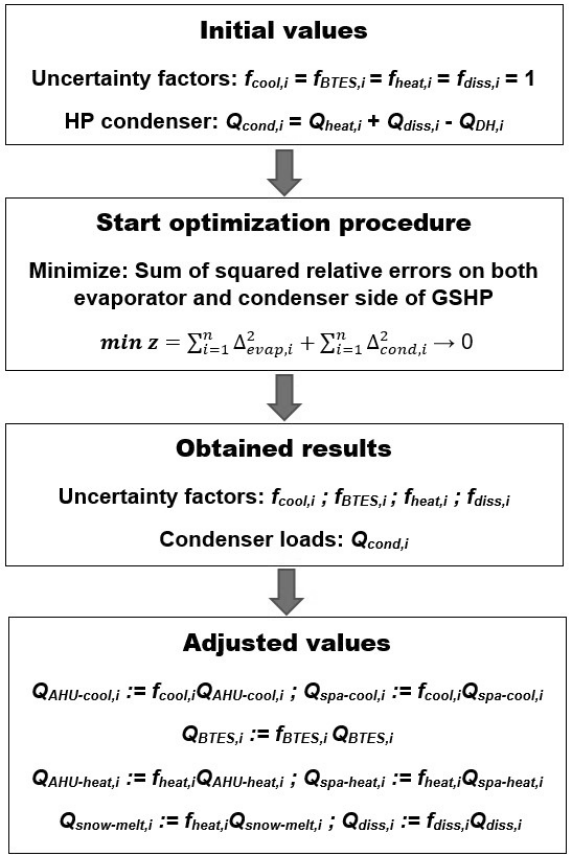

Figure 10. Procedure for data management.

2.2.3 Measured performance factors (PF)

There is no possibility to separately measure GSHP compressor and HP internal circulation pumps. Therefore, the adopted logical Annex 52 boundary schema for performance factors (PF) is PF H2/C2, defined as follows:

$$PF\ (H2) = \frac{\sum Q_{net\_heat}}{\sum W_{HP,hea} + \sum W_{CP,BTES,hea}} = \frac{\sum Q_{heat} - \sum Q_{DH,heat}}{\sum W_{HP,heat} + \sum W_{CP,BTES,heat}} \quad (10)$$

$$PF\ (C2) = \frac{\sum Q_{cool}}{\sum W_{HP,cool} + \sum W_{CP,BTES,cool}} \quad (11)$$

$$PF\ (HC2) = \frac{\sum Q_{cool} + \sum Q_{heat} - \sum Q_{DH,heat}}{\sum W_{HP} + \sum W_{CP,BTES}} \quad (12)$$

where $\sum Q_{\text{cool}}$, $\sum Q_{\text{heat}}$ and $\sum Q_{\text{DH,heat}}$ are the sum of loads for cooling, heating and DH, respectively over the studied period

$\sum W_{\text{HP}}$ and $\sum W_{\text{CP,BTES}}$ are the sum of GSHP and BTES circulation pumps power demands over the studied period. Additional indices indicate the allocation of power demands for heating and cooling, respectively.

Additionally, the heat pump measured COP is calculated according to the following relation:

$$COP\ = \frac{\sum Q_{HP,cond}}{\sum W_{HP}} \quad (13)$$

where $\sum Q_{HP,cond}$, and $\sum W_{HP}$ are the sum of thermal output of HP condenser and HP power demand (including HP compressor power input, internal energy use and internal circulation pumps).

Furthermore, the measured COP is compared to the calculated theoretical Lorentz/Carnot COP based on HP sink and source temperatures:

$$COP_{Lor} = \frac{\eta_{Lor} T_{lm,H}}{T_{lm,H} - T_{lm,L}} \quad (14)$$

$$\text{where } T_{lm,H} = \frac{T_{HPC,S} - T_{HPC,R}}{ln\left(\frac{T_{HPC,S}}{T_{HPC,R}}\right)};\ T_{lm,L} = \frac{T_{HPE,O} - T_{HPE,I}}{ln\left(\frac{T_{HPE,O}}{T_{HPE,I}}\right)}$$

$$COP_{Car} = \frac{\eta_{Car} T_{HPC,S}}{T_{HPC,S} - T_{HPE,I}} \quad (15)$$

$T_{lm,H}$ and $T_{lm,L}$ are the logarithmic mean temperature of the heat pump´s condenser and evaporator respectively. T_{HPC} and T_{HPE} are condenser and evaporator temperatures, while index notations I/O stand for inlet/outlet temperatures of the evaporator and S/R stand for supply/return temperatures of the condenser (expressed in Kelvin). The adopted values for Lorentz/Carnot efficiencies η_{Lor}/ η_{Car} in **Publication 3** are 0.39 and 0.43 respectively.

2.3 Modeling of the effective thermal resistance of groundwater-filled boreholes

Publication 4 is based on the data gathered from Aalto New Campus Complex (ANCC) and its GSHP-BTES energy system, introduced in detail in the previous section and **Publication 3**. Its 0.8 MW_{th} GSHP is connected to an irregular BTES field composed of 74 40mm-single-U groundwater-filled boreholes. All boreholes are connected in parallel, and their location / nomenclature is depicted in Figure 11 (boreholes highlighted in yellow belong to the DTS monitoring system). All 74 boreholes are drilled in hard rock (granite) with negligible fracturing; therefore, groundwater advection has been neglected (heat is transferred to the ground dominantly by conduction). The most relevant properties of the ANCC borehole heat exchanger (BHE) are summarized in Table 10.

Table 10. Aalto New Campus Complex BHE.

Number of boreholes within the irregular field	74
Borehole average depth, [m]	310.3
Borehole average effective depth, [m]	301.7
Borehole filling	Groundwater
Brine fluid type	28% ethanol-water
Borehole diameter, [mm]	115
U-pipe diameter / wall thickness, [mm]	40/2.4
U-pipe shank spacing (center to center), [mm]	60
Ground type	Granite
Ground thermal conductivity, [W/m.K]	3.3
Ground thermal diffusivity, [10^{-6} m^2/s]	1.2
Average undisturbed ground temperature, [°C]	8.7

Geological Survey of Finland (GTK) has installed the ANCC DTS monitoring system and is currently conducting the recording and data processing of the DTS measured data. Aalto University Campus & Real Estate (ACRE) is the owner of all data related to Aalto New Campus Complex and its energy system (including DTS data). There are six representative boreholes selected for DTS monitoring, two within each BTES group (A, B and C), namely: boreholes A6, A19, B7, B13, C8 and C20 highlighted in Figure 11.

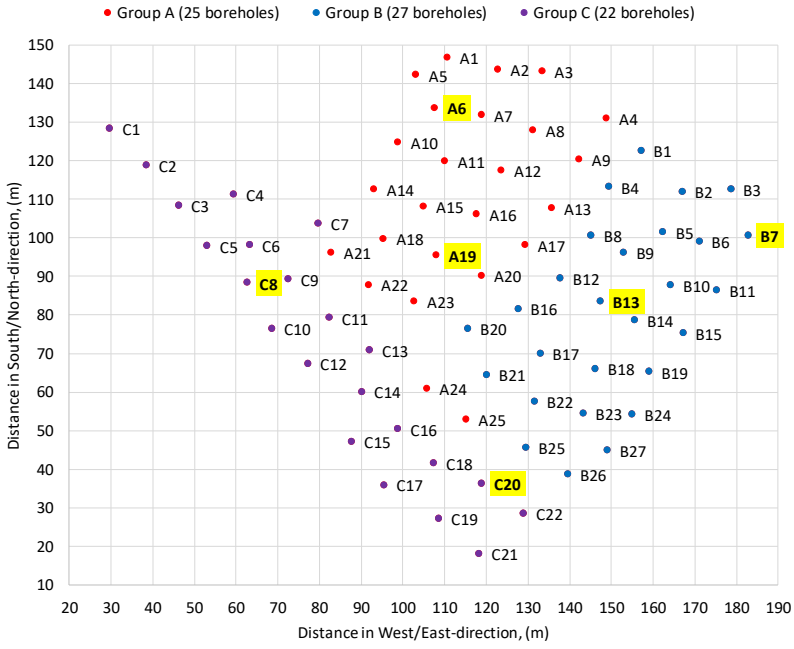

Figure 11. Aalto New Campus Complex borehole field.

2.3.1 Algorithm for the effective thermal resistance of groundwater-filled boreholes

Publication 4 presented two methods for deriving the effective thermal resistance (R_b*) from DTS temperature profiles of one representative borehole of the BTES field. They indirectly inferred borehole annulus temperature based on fluid inlet, bottom, and outlet temperatures. The first method estimated the fluid-to-water logarithmic mean temperature difference (LMTD) and the fluid-to-water heat transfer coefficient, and its discretization is based on the general approach for internal duct flow proposed by Incropera et al., (2007). The second method utilized the borehole wall temperature (determined indirectly from borehole annulus temperature) and is based on Hellström's formulation of borehole vertical profile developed by Lamarche et al., (2017). These two methos are detailly explained in **Publication 4** and would not be introduced in this summary. Instead, the algorithmic procedure for R_b* is presented below.

The procedure for estimating the effective thermal resistance R_b* of groundwater-filled boreholes is based on the recently developed correlations by Spitler et al., (2016a/b), according to the resistance scheme depicted in Figure 12 (all calculation formulas and correlations are detailly introduced in **Publication 4** and would not be repeated here).

The calculation of R_b* is based on iterative procedure since a priori film temperatures at the annulus and borehole wall are unknown. These temperatures influence the corresponding Rayleigh and Nusselt numbers and therefore, the resulting resistances of the annulus and borehole wall. This, in turn alters the local resistance R_b, the resistance between both legs R_{12}, total resistance R_a and also R_b* (depending on the adopted boundary condition mode). Finally, the iterative change in R_b* would also alter borehole wall temperature and the annulus temperature. The algorithm can stop when R_b* change is small, less than a pre-established threshold.

The input parameters of the algorithm are the pumping flow rate, heat rate per meter of borehole, mean fluid temperature and the chosen boundary condition mode - uniform borehole wall temperature (UBW) or uniform heat flux (UHF), and the calculation procedure is summarized as Algorithm 1 shown below.

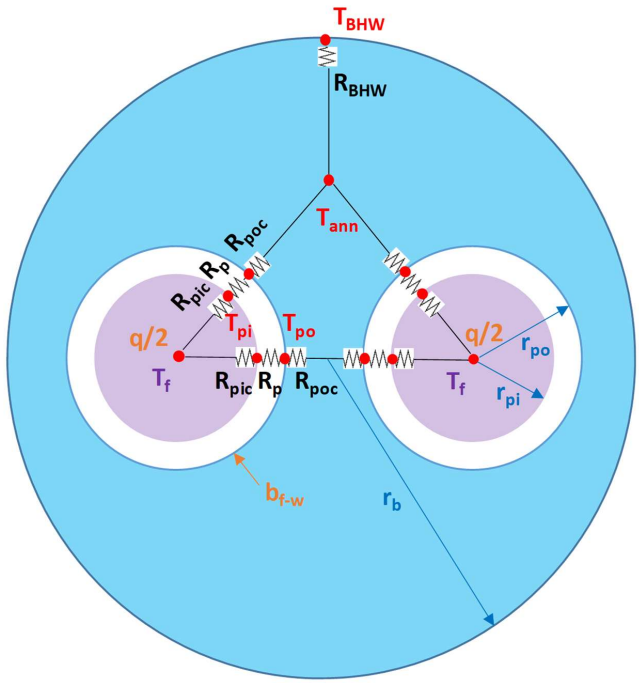

Figure 12. Resistance scheme of groundwater-filled boreholes.

Algorithm 1. Iterative algorithm for R_b* of groundwater-filled boreholes.

Input parameters: Pumping flow rate, heat rate per meter of borehole (q), mean fluid temperature (T_f), boundary condition mode (UBW/UHF)

1. **Calculate** pipe internal convective resistance R_{pic}, fluid properties evaluated at mean fluid temperature T_f
2. **Calculate** pipe wall conductive resistance R_p
3. **Calculate** water temperature at pipe outer wall T_{po}
4. **Assign** initial guess values for R_b* (0.15) and R_b (0.1)
5. **Calculate** initial values of borehole wall temperature T_{BHW} and annulus temperature T_{ann} (as an average of pipe outer wall and borehole wall temperatures)
6. **Start iteration loop:**
   a. **Evaluate** water properties at outer wall film temperature (average of T_{po} and T_{ann}) and calculate the convective resistance at outer wall R_{poc}
   b. **Evaluate** water properties at borehole wall film temperature (average of T_{ann} and T_{BHW}), calculate the convective resistance at borehole wall R_{BHW}
   c. **Calculate** resistances R_b, R_{12} and R_a
   d. **Calculate** R_b* depending on boundary condition mode (UBW/UHF)
   e. **Update** borehole wall temperature T_{BHW} and annulus temperature T_{ann}
7. **Exit loop** if absolute relative change of R_b* is less than a threshold (10^{-5})

2.3.2 Implementation and modeling of the BTES field

The presented methodology and algorithm have been implemented within the open-source toolbox for GHE simulation *Pygfunction* (Cimmino et al., 2018). Cimmino's versatile python application is based on the finite line source model (FLS) and can handle irregular configurations of multiple boreholes with hourly-based timestep. Another important feature implemented in these last versions of *Pygfunction* is the inclusion of a new module to evaluate fluid properties using *CoolProp* (Bell, 2021). This fluid module is directly used by the algorithm for R_b* calculation of groundwater-filled boreholes, while water properties at the pipe outer wall and borehole wall are evaluated using the external python package of *IAPWS* standard (Romera, 2021) and its *_Liquid module*.

The proposed enhancement of *Pygfunction* is applied with daily update of the effective thermal resistance R_b* calculated for groundwater-filled boreholes. For each timestep, the algorithm for R_b* is executed twice – for each one of the boundary conditions UBW/UHF – and finally the average of the two outcomes is taken, as suggested by Spitler and Javed (2016a). The enhanced *Pygfunction* simulation is finally used for validation against measured fluid temperatures of the initial 39 months of system operation. It is also compared with alternative *Pygfunction* simulations where the value of R_b* is constant, calculated with the multipole method (Claesson et al., 2011; Javed and Claesson, 2017) for grouted boreholes used by default in *Pygfunction*. Root mean squared error (RMSE) is the metric used for comparing simulation vs. measured data.

3. Results

The most relevant findings and results are introduced in this chapter. **Publications 1 and 2** presented a techno-economic analysis of GSHP-ATES operation and their long-term impact on the aquifer.

Publication 3 dealt with retrieving and managing of measured data of complex GSHP-BTES system, analysis of relevant performance indicators and measures for improving system operation, while **Publication 4** presented monitoring data of groundwater filled boreholes, studied the effective borehole thermal resistance in real operation and compared the modeling of the BTES field with the initial tree years of system operation.

3.1 Techno-economic analysis of GSHP-ATES operation

The technical parameters of ATES operation for both case studies (**Publications 1 and 2**) are shown on an annual basis in Table 11.

Table 11. Annual technical analysis of GSHP-ATES systems.

Relevant parameters of ATES operation	Publication 1 (Pukkila case study)	Publication 2 (Turku case study)	
		Scenario 1	Scenario 2
1-stg-cooling/heating/2-stg-cooling power, MW	1.75/0.35/-	-/1.43/1	0.3/1.63/1.3
Average water flow, m^3/day	1,283	2,492	2,496
Average abstraction temperature, ºC	6.3	10	10
Average injection temperature, ºC	3.7	10	10
Average temperature before GSHP, ºC	8.3	10	11.5
Average temperature after GSHP, ºC	3.7	2.1	2.5
Average GSHP supply temperature, ºC	58.9	65.4	66.5
Average DH return temperature, ºC	40	40.9	40.9
Average GSHP COP (heating mode)	3.4	3.14	3.21
Heating demand, MWh	7,749	67,971	
Heat demand covered by GSHP, MWh	2,923	12,315	13,882
Heating demand covered by GSHP, %	38 %	18 %	20 %
Cooling demand, MWh	1,840	12,382	
First stage cooling covered, MWh	1,840	-	1,605
Second stage cooling covered, MWh	-	8,331	8,006
Total cooling demand covered, MWh	1,840	8,331	9,611
Total cooling demand covered, %	100 %	67 %	78 %
Electricity demand (GSHP), MWh	882	3,934	4,335
Electricity demand (ATES pump.), MWh	142	275.6	276.1
Electricity demand (HP-DH pump.), MWh	-	57.7	62.1
Electricity demand (HP-DC pump.), MWh	-	130.7	150.5
Total electricity demand, MWh	1024	4,398	4,823

In **Publication 1**, even with 11% of peak heat power, the GSHP covered roughly 38% of the annual heating demand. In **Publication 2**, with 5-6% of peak heat power respectively for Scenario 1-2, the GSHP supplied some 18-20% of the annual heating demand. Moreover, a significant improvement in Scenario 2 is achieved when comparing the cooling demand covered by ATES. The scheme with two cooling exchangers in Scenario 2 supplied 78% of DC demand annually (compared to 67% of Scenario 1), from which the first stage cooling represent roughly 1/6.

The economic evaluation of both case studies regarding the investment costs and the energy production cost are presented in Table 12 and Table 13, respectively. In **Publication 1**, the investment costs do not include the necessary DC network implementation, and the resulted overall energy production cost is slightly over 40 €/MWh. The total investment cost is roughly 1.06 million € from which 22% correspond to HP / exchangers and 75% is related to the underground part (wells, pipes). In **Publication 2**, the energy production cost is close to 30 €/MWh. Overall investment cost is around 2.3 million €: 26% correspond to GSHP / exchangers and 73% is related to the underground components (connection pipes and wells). These figures, in both case studies, are in line with the research of Schüppler et al., (2019), where similar ATES system in Germany resulted in total investment cost of roughly 1.28 million € from which 23% correspond to HP / exchangers and 60% is related to wells / piping. Additionally, Todorov et al., (2020) achieved an important -4% reduction of ATES pumping flow (with similar production cost below 30 €/MWh) by multi-objective optimization of ATES flow rate and the specific energy consumption of GSHP compressor and ATES pumping.

Table 12. Economic evaluation of GSHP-ATES systems.

Investment cost	**Publication 1 (Pukkila case study)**	**Publication 2 (Turku case study)**	
		Scenario 1	**Scenario 2**
Preliminary subsurface studies, pumping tests and geological report, €	30,000 €	30,000 €	30,000 €
Ground source heat pump, €	175,000 €	429,000 €	489,000 €
Heat exchangers, €	61,250 €	85,050 €	111,300 €
Pumping wells (incl. pump and equipment), €	680,000 €	1,360,000 €	1,360,000 €
Underground connection pipes PEHD, €	110,000 €	325,000 €	325,000 €
Total investment cost, €	**1,056,250 €**	**2,229,050 €**	**2,315,300 €**

Table 13. Energy production cost of GSHP-ATES operation.

Annuity method	**Publication 1 (Pukkila case study)**	**Publication 2 (Turku case study)**	
		Scenario 1	**Scenario 2**
Total investment cost, €	1,056,250 €	2,229,050 €	2,315,300 €
Annuity factor (interest rate 5%, lifetime 20 years)	0.0802		
Annual investment cost, €	84,756 €	178,865 €	185,786 €
Annual fiixed O&M cost, €	10,563 €	22,291 €	23,153 €
Annual energy cost (electricity), €	102,373 €	439,820 €	482,317 €
Total annual cost, €	197,692 €	640,976 €	691,256 €
Cost per MWh of heating / cooling energy	**41.51 €**	**31.05 €**	**29.43 €**

3.2 Long-term impact on the aquifer

3.2.1 Reversible (summer/winter) ATES operation

The simulation of the thermal front of ATES operation (**Publication 1**) for year 1, 2, 4, 8 and 20 is presented in the following Figure 13, for the week when the cold and warm plumes achieve their maximum expansion. Both wells are represented by a 50x50m pink cell. Left images depict the maximum annual cold well plume expansion (end of the winter period, after week 11), while right images are the maximum annual warm well thermal plume expansion (end of the summer period, after week 31).

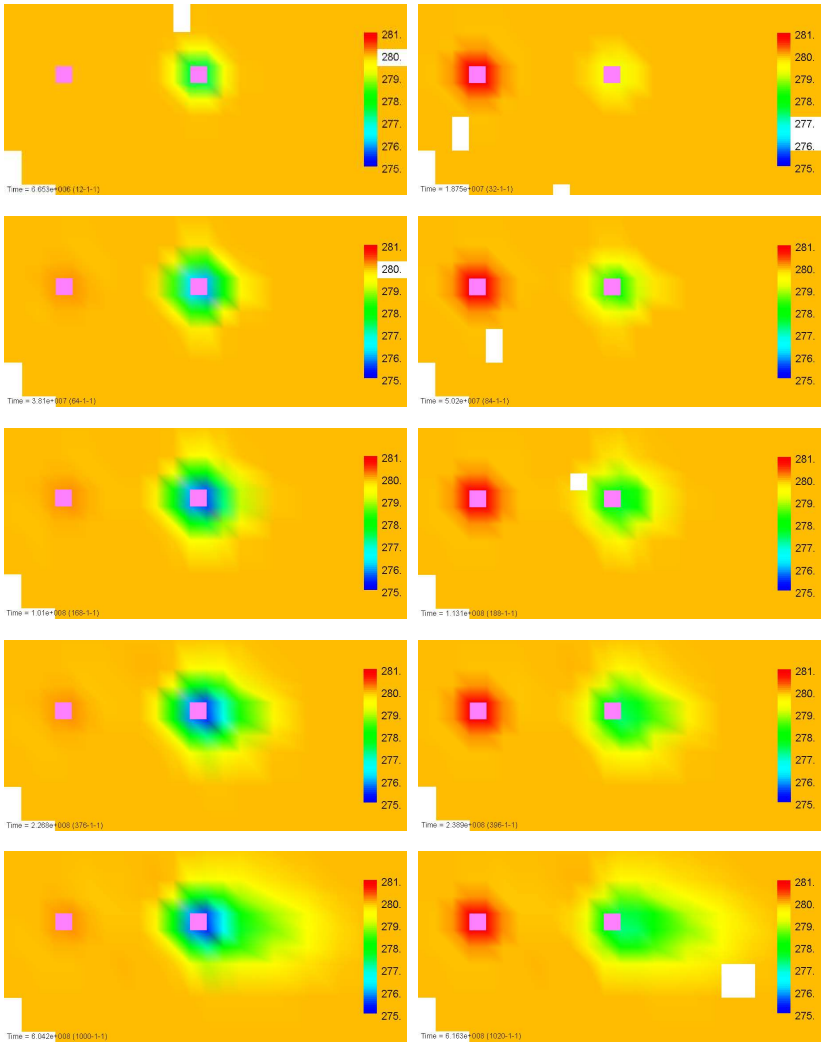

Figure 13. Long-term aquifer thermal field evolution (in rows: years 1, 2, 4, 8 and 20; left column: end of winter; right column: end of summer; temperature scale in Kelvin).

It can be observed that the thermal plume of the warm well maintains more or less within its thermal radius (**Publication 1**) of roughly 75 m, since the heat injected in the aquifer is less compared to the heat abstracted from it. Moreover, the heat plume around the warm well almost vanishes at the end of the winter period (left hand side images), while the plume around the cold well increases slowly over the years. After 20 years of ATES operation, the thermal plume of the cold well expands several hundreds of meters to the south-east, following the dominant groundwater flow direction. All in all, it can be concluded that the locations of the wells (cold well located downstream) and the distance between them (around three times their average thermal radius) is favorable for a correct and efficient long-term ATES operation.

3.2.2 One-way ATES operation

In **Publication 2**, although the undisturbed aquifer temperature is as high as 10°C, first stage cooling (in Scenario 2) can be used 8736 out of 8760 hours annually, and it represents 17% of the cooling demand covered by GSHP. This configuration also increases the temperature before GSHP evaporator by 1.5°C on average, which improves the COP and enhances heat pump´s capacity in the evaporator as well. The average injection temperature lays in a narrow range of roughly 10 ±1 °C, which justifies a one-way ATES operation and consequently, the thermal impact on the aquifer remains very limited. The simulation results after 20 years of one-way operation are presented in Figure 14, where hydraulic head is represented by iso-lines with resolution of 0.25 m. In order to mitigate the hydraulic impact of pumping, injection well is placed downstream while abstraction well is located upstream (Figure 14).

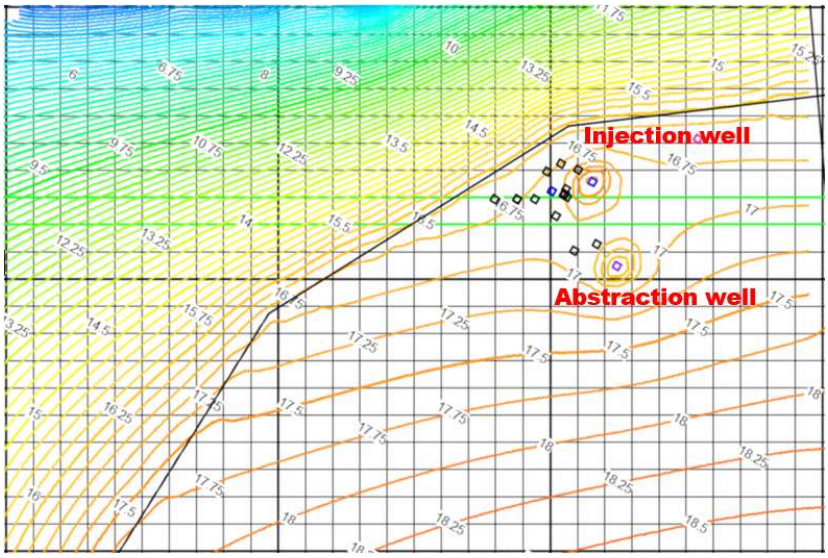

Figure 14. Hydraulic impact after 20 years of one-way ATES operation.

The maximum simulated drawdown (within a 100x100m well cell) is 1.28/1.17 m in summer/winter, respectively, which corresponds to 5.0/4.7 m inside the pumping well (well radius 0.4 m). The overall impact of ATES pumping vanishes in about 500 m from each well, thus it is not affecting in significant way the surrounding groundwater areas.

3.2.3 Temperatures' analysis of system operation

Scenario 2 of **Publication 2** is investigated more detailly, as follows. GSHP COP is 3.2 on average, slightly improved to 3.3 during the winter due to lower GSHP supply temperature (64°C on average), while during the summer GSHP covers higher heat fraction and the average supply temperature increases to 69°C (see Figure 15).

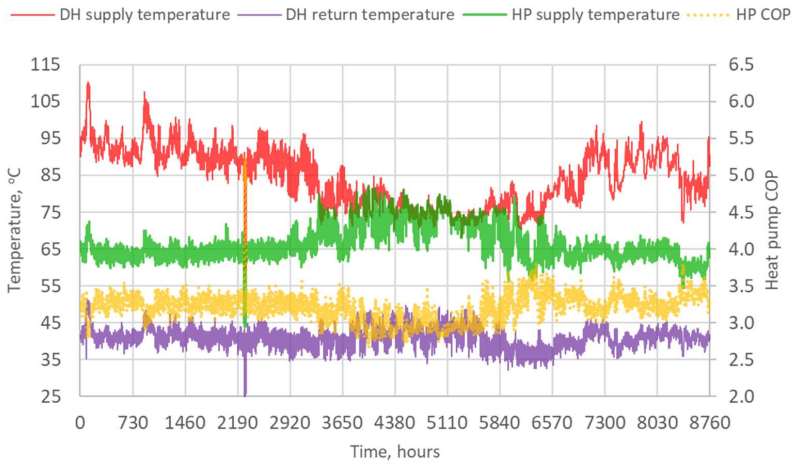

Figure 15. Annual evolution of DH/GSHP network temperatures.

GSHP-ATES operation is based on energy conversion using electricity to cogenerate heating and cooling in a single process. GSHP is the principal electricity consumer accounting for 90% of the annual demand, followed by ATES pumping (6%) as well as pumping needed to inject HP´s supply energy to DH / DC networks – respectively 1% / 3%. This is important to be acknowledged since total electricity demand (4.8 GWh/a) has significant impact on the annual cost and, consequently on the specific cost of generated heating and cooling energy, as seen in Table 13.

ATES system is well balanced, as seen from the average injection and abstraction temperatures equal both to aquifer´s undisturbed temperature of 10°C. Moreover, the system is balanced in terms of energy, as shown in Table 11, since the annually covered heat demand is equal to the supplied cooling plus GSHP power demand (13.9 GWh). In Figure 16 is depicted the annual variation of all temperatures along ATES flow-path: abstraction, after first stage cooling, after GSHP evaporator and finally injection.

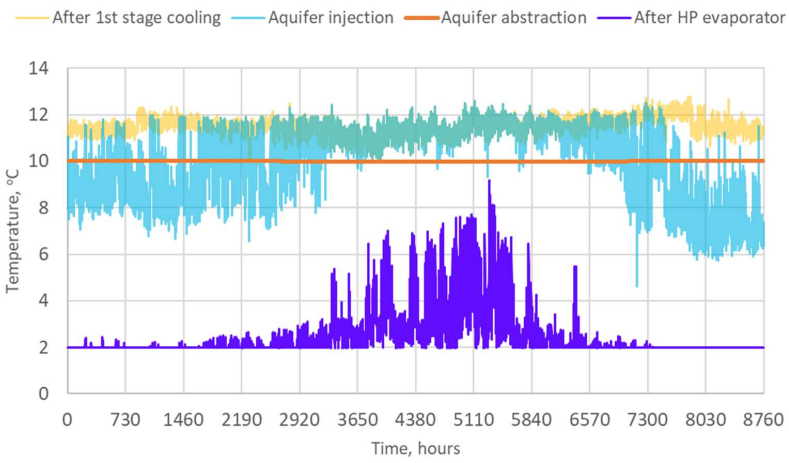

Figure 16. Annual evolution of ATES temperatures.

3.2.4 Sensitivity analysis of GSHP-ATES operation

About 70% of the energy production cost is related to electricity consumption, from which GSHP accounts for around 90% (Table 13). Heat pump´s COP is an important variable to consider in order to boost system´s efficiency and decrease cost. That is why, in **Publication 2**, a sensitivity analysis for Scenario 2 is performed, with four different values of the exponential parameter p: 0.2, 0.4, 0.6 and 0.8 corresponding to cases 1, 2, 3 (base case) and 4 respectively. By decreasing p, the average GSHP supply temperature also declines, while the average COP increases and the energy production cost is lower. The percentage variations compared to the base case 3 are plotted in Figure 17.

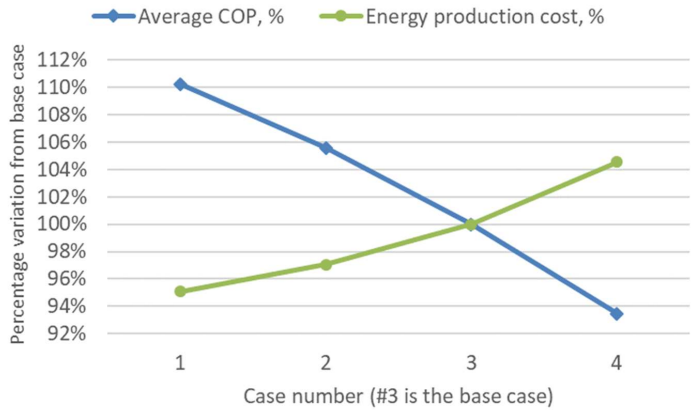

Figure 17. Sensitivity analysis: COP and energy production cost (case 3 = 100%).

3.3 DVR data management of a complex GSHP-BTES system

Publication 3 developed a specific data validation and reconciliation (DVR) procedure in order to handle the inherent uncertainty of all thermal energy meters. From raw measured data, it is not trivial to determine the evaporator and condenser loads of GSHP (not directly measured), fulfilling the energy balance on both sides of the heat pump. That is why the DVR methodology introduced in Section 2.2.1 and 2.2.2 was applied for managing the initial raw data by the introduction of daily uncertainty factors corresponding to cooling, BTES, heating and dissipation.

3.3.1 Results and analysis of the evaporator side

The results of the evaporator side between July 2019 and December 2020 are summarized in Table 14 and Figure 18. The total cooling loads from June to August 2020 account for almost 2/3 of overall annual cooling demand, while AHU-cooling demand over these three months is almost half of annual cooling loads. On the other hand, from October 2019 to April 2020 there is no AHU-cooling demand at all, although space cooling is needed during the whole year. Therefore, it can be concluded that summer operation lasts roughly for three months (June, July and August) while winter mode covers seven months between October and April, with two transition months in between (May and September).

Similarly, heat from the BTES field is heavily extracted from October 2019 to April 2020 (again, May and September are transition months with lower extraction activity), whereas heat injection occurs during the summer months of June, July and August. Overall, the hourly calculated imbalance ratio during the last 12 months is 7 (1869 MWh heat extraction / 268 MWh heat injection). Thus, the interactions with the BTES field are not balanced which can potentially lead to its overcooling in the long term. The uncertainty factors for cooling and BTES are still far from 1 from July to September 2019 and the standard deviation is high (Table 14). After that they are more stable, i.e., close to 1 and with low standard deviation (due to testing of thermal energy meters April and May 2020 are exceptions).

Table 14. Data management: Results of the evaporator side.

Month / Year	Average outdoor temp.[°C]	AHU cooling [MWh]	Space cooling [MWh]	Total cooling [MWh]	Average cooling factors (± stdev)	BTES [MWh]	Average BTES factors (± stdev)	Evaporator [MWh]
Jul 2019	17.9	-108.8	-54.7	-163.5	1.36 ±0.20	64.3	0.73 ±0.20	99.5
Aug 2019	17	-58.4	-57.2	-115.7	1.36 ±0.49	67.9	0.63 ±0.17	47.8
Sep 2019	11.4	-11	-38.2	-49.2	1.10 ±0.15	-56.8	0.92 ±0.20	106.4
Oct 2019	5.2	0	-28.8	-28.8	1.01 ±0.01	-202	1.06 ±0.03	230.8
Nov 2019	1.9	0	-22	-22	1.00 ±0.00	-268.5	1.07 ±0.02	290.6
Dec 2019	1.3	0	-15.5	-15.5	1.00 ±0.00	-279.9	1.06 ±0.02	295.4
Jan 2020	1.7	0	-16.2	-16.2	1.00 ±0.00	-274.7	1.06 ±0.02	290.9
Feb 2020	0.3	0	-18.5	-18.5	1.00 ±0.00	-265.6	1.06 ±0.02	284.1
Mar 2020	1.6	0	-20.5	-20.5	1.00 ±0.00	-266.3	1.06 ±0.02	286.8
Apr 2020	4.6	0	-24.2	-24.2	1.02 ±0.04	-224.7	1.11 ±0.04	249
May 2020	9.5	-7.7	-36.7	-44.4	1.07 ±0.08	-116.4	1.11 ±0.10	160.9
Jun 2020	18.6	-135.1	-41.4	-176.5	1.02 ±0.07	86.6	0.99 ±0.04	89.8
Jul 2020	16.8	-74.6	-35	-109.6	1.03 ±0.07	49.6	0.98 ±0.05	60
Aug 2020	17	-92	-36.1	-128.1	1.04 ±0.07	64.6	0.99 ±0.04	63.6
Sep 2020	12.9	-4.5	-32.8	-37.3	1.04 ±0.05	-28.6	1.01 ±0.05	65.9
Oct 2020	8.3	-0.1	-32.5	-32.6	1.01 ±0.01	-122.8	1.03 ±0.03	155.4
Nov 2020	4.3	0	-30.6	-30.6	1.00 ±0.00	-206.1	1.03 ±0.02	236.7
Dec 2020	0.8	0	-30.9	-30.9	1.00 ±0.00	-297	1.02 ±0.02	327.8
Last 12 months	8	-314	-355	-669	1.02 ±0.05	-1601	1.04 ±0.06	2271

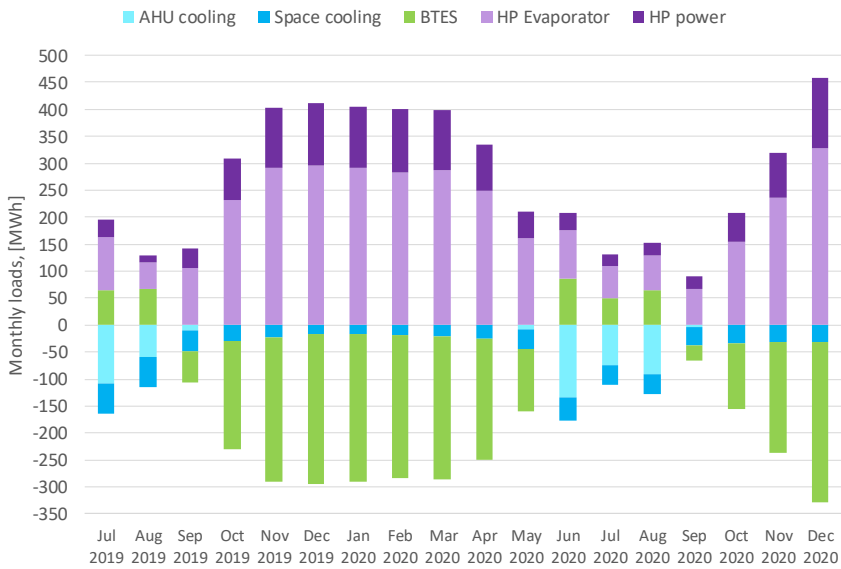

Figure 18. Monthly loads on the evaporator side.

The symmetry of Figure 18 also reflects the balance of all loads on the evaporator side. In summer, BTES loads injected into the ground (ground acting as heat sink) plus HP evaporator balance out all cooling loads. The rest of the year (from September to May) evaporator loads are balanced out by total cooling and BTES loads extracted from the ground (being the ground used as heat source).

3.3.2 Results and analysis of the condenser side

The monthly loads on the condenser side are presented in Table 15 and Figure 18. In Figure 18, condenser and DH loads are shown as negative in order to highlight the symmetry with all heating and dissipation loads due to the energy balance. As mentioned previously, winter mode can be clearly observed from October 2019 to May 2020, accounting for over 90% of annual heating demand and HP condenser loads. Moreover, space- and AHU-heating demand is more or less evenly distributed over the year, while snow melting is practically inexistent.

As expected, dissipation loads are realized almost entirely during the summer operation in June, July and August, when they impact hugely in the energy balance of the condenser side (Figure 19). Similarly, the symmetry of Figure 19 highlights the energy balance on the condenser side of the heat pump: heat input is provided by the GSHP condenser and DH balanced out by total heating output and dissipation loads (in summer, acting as heat sink). Overall, the GSHP is utilized very intensively covering some 95% of total annual heat input, DH accounting only for 5%. However, the past winter (2019-2020) was exceptionally mild in Finland (YLE, 2021), thus probably in normal meteorological conditions, the share of DH of overall annual heat input is expected to be higher.

Table 15. Data management: Results of the condenser side.

Month / Year	Condenser [MWh]	AHU heating [MWh]	Space heating [MWh]	Snow melting [MWh]	Total heating [MWh]	Average heating factors (± stdev)	DH for heating [MWh]	Dissipation [MWh]	Average dissipation factors (± stdev)
Jul 2019	132.1	19.3	21.6	0	40.9	0.99 ±0.29	8.8	99.8	0.96 ±0.07
Aug 2019	62.1	19.4	21	0	40.4	1.03 ±0.11	8.6	30.4	1.04 ±0.19
Sep 2019	141.1	66.4	78.7	0	145.1	0.97 ±0.10	10.2	6.7	1.01 ±0.07
Oct 2019	309.6	177.5	143.1	0.2	320.9	0.95 ±0.02	12.2	0.9	1.00 ±0.00
Nov 2019	402.2	252.6	171.7	1.6	425.8	0.95 ±0.01	23.8	0.1	1.00 ±0.00
Dec 2019	410.9	251.6	177	2.6	431.2	0.96 ±0.02	20.3	0	1.00 ±0.00
Jan 2020	404.8	239.7	178.9	1.9	420.4	0.96 ±0.01	15.7	0	1.00 ±0.00
Feb 2020	400.2	257.1	167.9	2	427	0.95 ±0.02	26.8	0	1.00 ±0.00
Mar 2020	398.9	248.1	164.6	0.8	413.4	0.96 ±0.01	14.5	0	1.00 ±0.00
Apr 2020	334.3	196.2	148	0.1	344.3	0.92 ±0.03	10	0.1	1.00 ±0.00
May 2020	210.6	107.5	113	0	220.5	0.90 ±0.07	10.1	0.7	1.00 ±0.00
Jun 2020	122.5	21.8	17.8	0	39.7	0.99 ±0.05	9.5	92.3	1.00 ±0.01
Jul 2020	82.3	19.3	32.9	0	52.2	1.02 ±0.19	9.6	39.6	1.00 ±0.01
Aug 2020	87.2	19	28.8	0	47.8	0.98 ±0.03	9.6	49	1.00 ±0.01
Sep 2020	90	36.1	63	0	99.1	0.97 ±0.05	9.4	0.4	1.00 ±0.00
Oct 2020	208.1	112.2	105.9	0	218.1	0.98 ±0.03	10	0	1.00 ±0.00
Nov 2020	320.1	147.5	183.9	0	331.4	0.98 ±0.02	11.3	0	1.00 ±0.00
Dec 2020	457.7	196.1	297.1	1.5	494.7	0.98 ±0.01	37	0	1.00 ±0.00
Last 12 months	3117	1600	1502	6	3109	0.97 ±0.07	173	182	1.00 ±0.00

Overall, the uncertainty factors for heating and dissipation are close to 1. However, from July to September 2019 their standard deviation is high (Table 15). After that, the factors are quite stable, close to 1 and with low standard deviation. All thermal energy meters were tested in April and May 2020 while space-heating meter presented malfunctioning during several days of July 2020 - that is the reason for higher discrepancies during these periods.

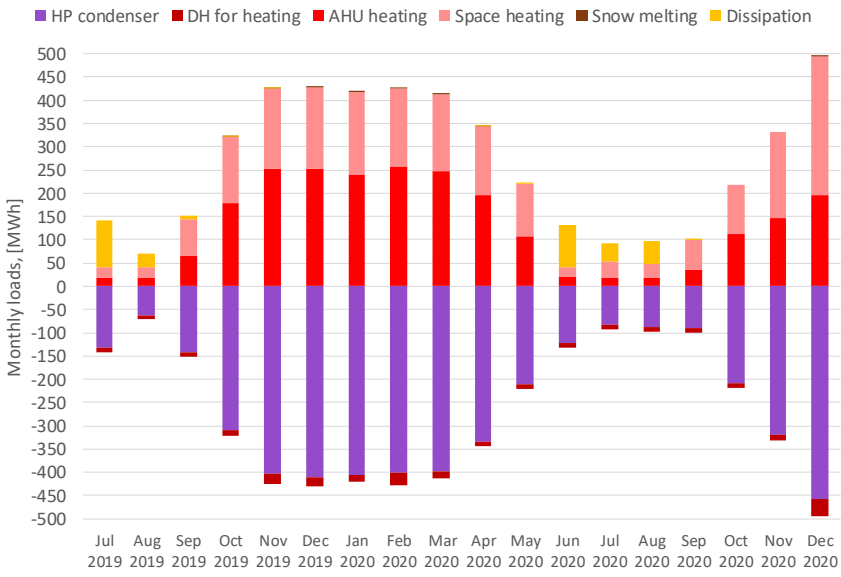

Figure 19. Monthly loads on the condenser side.

3.3.3 Performance of the GSHP energy system

Monthly Seasonal Performance Factors (SPF) with Annex 52 schema (boundary 2) are calculated: heating (SPF-H2), cooling (SPF-C2) and combined SPF-HC2 factors are shown in Figure 20, as well as the heat pump measured COP.

Cooling SPF factors increase greatly during the winter period (between 50 and 70) due to a direct free-cooling from the ground supplied as space-cooling. However, space-cooling demand in winter is a tiny share of annual cooling demand (Figure 18). As expected, winter SPF-H2 is lower than HP COP since the former accounts for BTES circulation pumps. The SPF-H2 factor also takes into account the net heating demand which in winter is a difference between HP condenser and DH input (there is no dissipation), while heat pump COP is the ratio between condenser output and HP power input.

During the summer months (June, July and August) SPF-C2 is lower, between 6.2 and 7.3. Heat pump is intensively utilized to meet almost half of all summer cooling loads, providing active AHU-cooling and simultaneously enhancing the effect of “free heating” on the condenser side. That is why summer SPF-H2 factors are higher than HP COP (Figure 20). Overall, some two-thirds of annual cooling demand is generated by free-cooling (assuming all space-cooling as “free-cooling” provided by the ground source).

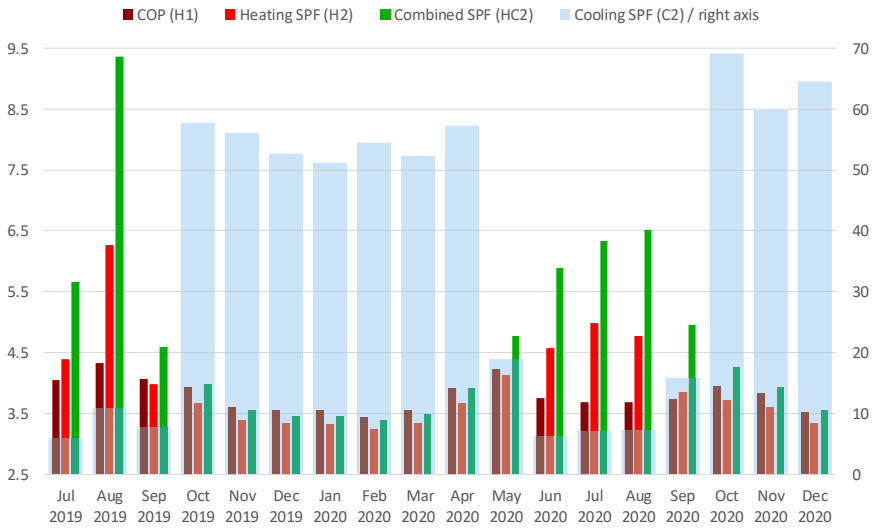

Figure 20. Monthly performance factors for system boundary H2/C2/HC2 and heat pump COP.

The overall heat pump COP, SPF factors for heating, cooling and combined (system boundary 2) are respectively 3.7, 3.5, 9.3 and 4.0 for the entire period (July 2019 – December 2020), while the annualized values over the first evaluation period (October 2019 - September 2020) are respectively 3.7, 3.5, 9.3 and 3.9. For comparison, Spitler & Gehlin (2019) reported 3.6 and 6.4 as median values for SPF-H2 and C2, respectively, in their exhaustive overview of long-term measured performance of 55 GSHP systems. They also provided values of 3.7 (H2) and 27 (C2) for their own case study: the new student center at Stockholm University in Sweden (Spitler & Gehlin, 2019). The latter factor (C2) is so high because cooling was supplied entirely as free-cooling from the ground peaking in winter between 40 and 60, since source CPs were proportionally allocated to the supplied heating and cooling loads (similarly to the present case study). Another recent study (Bockelmann & Fisch, 2019) presented an 8/10-year performance of two GSHP-BTES office buildings in Germany, reporting 2.6 and 4 as average SPF H2 and C2 respectively. Similar research of a 4-year GSHP-BTES performance in a German office reported 3.8 and 8 as typical heating SPF H2 and typical cooling SPF C2, respectively (Luo et al., 2015).

3.3.4 Heat pump COP and summer performance gap

It is important to acknowledge that heat pump COP depends on both temperatures on the evaporator side (heat source) and the condenser side (heat sink). GSHP fluid temperatures on both sides are plotted in Figure 21, where also the measured vs. expected Lorentz/Carnot COP (calculated with Equations (14) and (15), and efficiencies η_{Lor}=0.39/ η_{Car}=0.43) are compared. Generally speaking, the higher the evaporator temperatures and the lower the condenser temperatures, the higher the COP and vice versa. During the winter period (October 2019 – May 2020), GSHP condenser must provide heating at higher temperatures (average supply/return 42/30°C), while the intensive heat extraction from the BTES field provokes temperature drop in the evaporator (average inlet/outlet 4/1°C). The calculated winter COP (orange line) fits well with the measured COP (green line) showing low plateau with minimum values around 3.5 between November 2019 and March 2020.

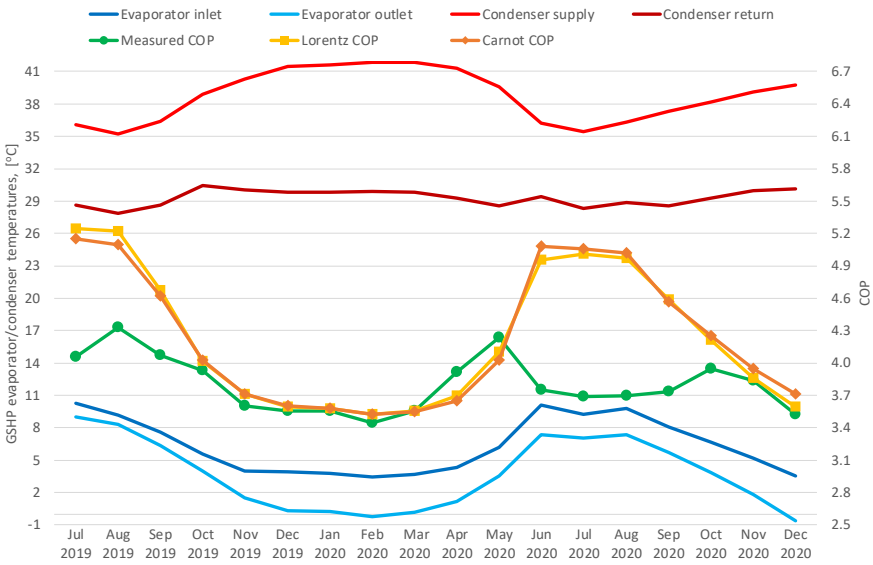

Figure 21. GSHP evaporator/condenser fluid temperatures and COP.

On the other hand, in summer operation (June, July and August 2020), GSHP condenser operates at lower temperatures (average supply/return 36/29°C) and the evaporator at higher (average inlet/outlet 10/7°C). This enhances the calculated summer COP to around 5. However, this theoretical expectation is not fulfilled by the measured COP (only 3.7, very similar to the average winter COP), presenting a huge gap between June and September (Figure 21).

3.3.5 Effect of GSHP partial load operation

The significant gap between measured COP and expected (calculated) COP in summer operation – as discussed in the previous section - probably might be provoked by the HP partial load operation. Several studies (Piechurski et al., 2017; Watanabe et al., 2009; Fahlén, 2012) concluded that heat pump COP is impacted by a partial load operation and highlighted that more frequent "on/off" switching can reduce HP efficiency (Piechurski et al., 2017). As mentioned previously, ANCC system´s operation is based on cascade launching of HP modules (from 1 to 9 units) and each module can be additionally adjusted to deliver a fraction between 0% and 100% of its nominal capacity. This effect of partial load operation is studied in Figure 22, where 366 daily based data points (representing the first evaluation period between October 2019 and September 2020) are plotted depending on the average daily percentage of HP operating modules. Data are additionally clustered in three groups: winter operation (258 days, ODA up to 12-14ºC), summer operation (78 days, ODA over 15ºC) and transition period (30 days, ODA 12-15ºC).

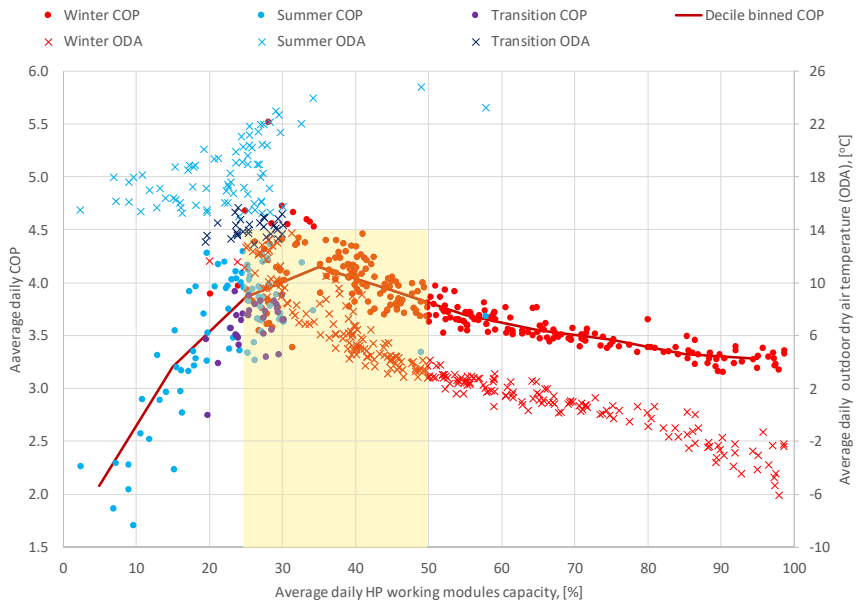

Figure 22. Heat pump COP and ODA in partial load operation.

In Figure 22, the average daily COP is plotted on the left axis while on the secondary (right) axis it is shown the average daily ODA temperature (with cruxes). During the winter period, HP COP steadily decreases as modules operate at higher rates (between 25 and 100%). In winter, heat pump COP is closely correlated to ODA temperature, which is expected, since COP is lower with colder weather (during the winter days with high heating demand, HP entering fluid temperature (EFT) is lower and HP supply temperature is higher, thus

COP goes down). In summer, when GSHP modules work at lower capacities of normally up to 30%, COP sharply decreases, especially for HP capacity below 10-15%. Eventually, a maximum COP (plotted as decile binned COP, brown line in Figure 21) is achieved between 25% and 50% of HP average capacity which mostly corresponds to the start / end period of heating operation (Figure 22, highlighted in yellow).

3.4 BTES model validation: initial 3 years of system operation

3.4.1 Estimation of BTES loads and pumping flow rate

The BTES loads between October 2019 and May 2021 are obtained using the specifically developed DVR methodology (**Publication 3**). Prior to this, BTES loads are estimated based on the pumping flow rates and measured inlet/outlet BTES temperatures. Following the methodology for data reconstruction introduced in **Publication 3**, it is possible to establish the following correlations between the pumping volume flow rate V_f (in l/s per borehole) and the frequency percentage signals (*FP1/FP2*) sent to each one of the twin BTES circulation pumps (CP):

$$Combined\ Frequency\ Factor: CFF = \sqrt[3]{\left(\frac{FP1}{100}\right)^3 + \left(\frac{FP2}{100}\right)^3}$$

$$Heat\ extraction: V_f = 0.4193 x CFF\ /\ Heat\ injection: V_f = 0.3519 x CFF \quad (16)$$

The resulting BTES loads and pumping flow rates (on a monthly basis) are shown in Figure 23.

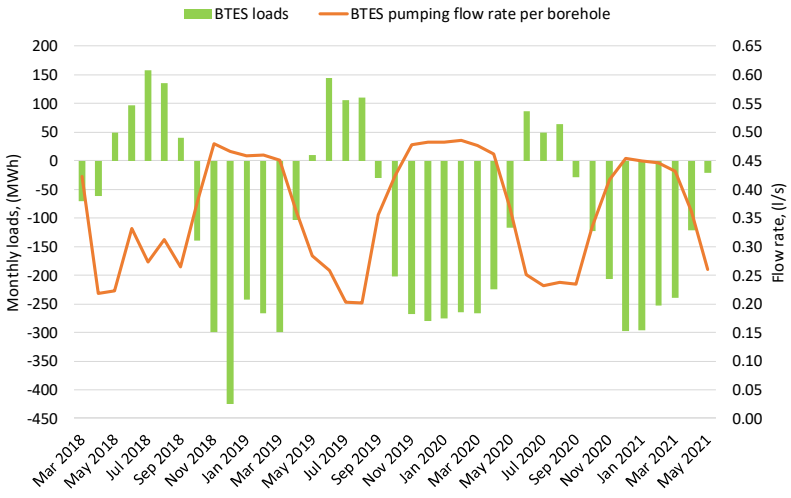

Figure 23. BTES loads and pumping flow rates (2018 – 2021).

3.4.2 Model validation of the BTES field

The developed models utilize daily based data (loads and pumping flows), as well as borehole field geometry and ground parameters according to Table 10. The different scenarios are listed below:

1. Measured data (mean fluid temperature)
2. Simulated: Algorithm for R_b* calculation of water-filled boreholes coupled with *Pygfunction* (with daily R_b* update, average R_b* = 0.22 m.K/W)
3. Simulated: *Pygfunction* modeling standard grouted boreholes, grout thermal conductivity k_g = 0.6 W/mK (constant R_b* = 0.18 m.K/W)
4. Simulated: *Pygfunction* modeling standard grouted boreholes, grout thermal conductivity k_g = 1.2 W/mK (constant R_b* = 0.13 m.K/W)
5. Simulated: *Pygfunction* modeling standard grouted boreholes, grout thermal conductivity k_g = 1.8 W/mK (constant R_b* = 0.12 m.K/W)

The results, using a 15-day moving average of the mean fluid temperature, in order to reduce the noise in data representation, are plotted in Figure 24.

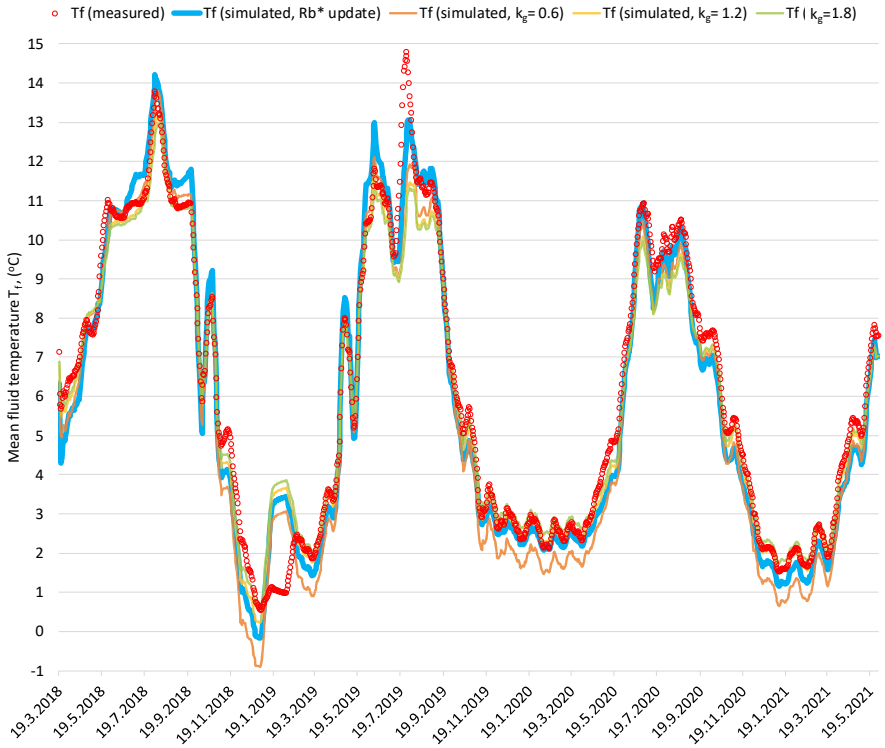

Figure 24. BTES model validation: measured mean fluid temperature vs. simulations.

The annual comparison metrics, developed as 365-day periods after the starting day (March 19th, 2018) are summarized below:

- Mean fluid temperature (annual and overall average)

- Temperature amplitude, difference between maximum and minimum fluid temperatures within the annual period (annual and overall average)
- Mean fluid temperature RMSE, compared with measurements (annually and overall)

The results are listed in Table 16 and the overall metrics' comparison depicted in Figure 25.

Table 16. BTES model validation: results comparison.

Scenario	Annual period	Average fluid temperature T_f, [°C]	Temperature amplitude, [°C]	T_f RMSE compared with measured, [°C]
1. Measured	2018	6.62	13.24	-
	2019	6.34	12.8	-
	2020	5.4	9.4	-
	Overall	6.12	11.81	-
2. Simulated (water-filled, R_b* update)	2018	6.74	14.37	0.92
	2019	6.16	11.5	0.6
	2020	4.89	9.77	0.56
	Overall	5.93	11.88	0.71
3. Simulated (grouted, k_g=0.6 W/mK)	2018	6.42	14.69	0.98
	2019	5.69	11.07	0.93
	2020	4.63	9.82	0.79
	Overall	5.58	11.86	0.9
4. Simulated (grouted, k_g=1.2 W/mK)	2018	6.69	12.93	0.85
	2019	5.97	9.7	0.82
	2020	4.99	8.61	0.54
	Overall	5.88	10.41	0.75
5. Simulated (grouted, k_g=1.8 W/mK)	2018	6.77	12.38	0.88
	2019	6.06	9.27	0.86
	2020	5.1	8.23	0.55
	Overall	5.98	9.96	0.78

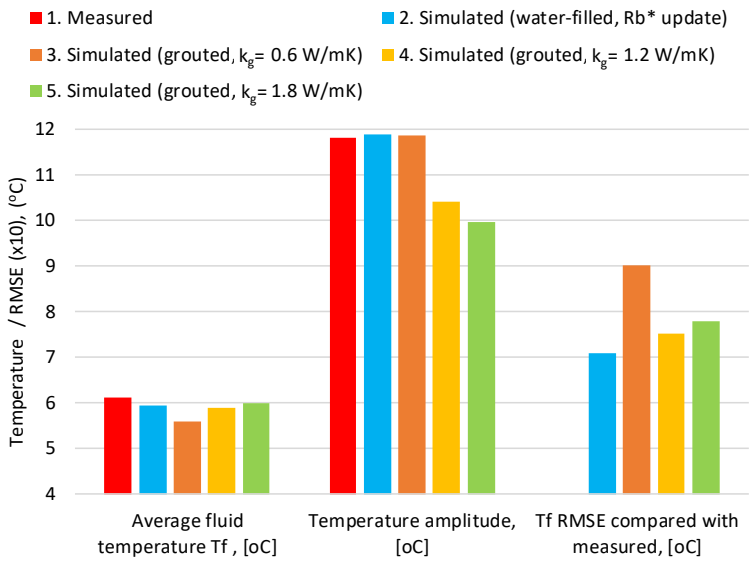

Figure 25. BTES model validation: overall comparison indicators.

The only significant deviation between measurements and simulation occurs between July 13th and 23rd, 2019 when the BTES circulation pumps had very low activity and the mean fluid temperature increased approaching the ambient temperature (Figure 24). The presented hybrid model (Scenario 2), enhancing the *Pygfunction* toolbox with capabilities to calculate the R_b* of groundwater-filled boreholes dynamically and updating it during the simulation, has shown very good agreement with measured data, even though the uncertainty of the estimation of BTES loads and flow rates before October 2019 is high. The model fits closely to measured data, which is reflected on its best comparison indicators: average fluid temperature, temperature amplitude of the annual cycle and RMSE (Figure 25). It is followed by Scenario 4 (k_g = 1.2 W/mK and constant R_b* = 0.13 m.K/W), however the latter differs from measurements in temperature amplitude. Similar value for grout thermal conductivity (k_g = 1.3 W/mK) is also suggested by Earth Energy Designer (EED, 2021a) when simulating groundwater-filled boreholes (EED, 2021b).

3.4.3 R_b* variability in real operation

The correlation of R_b* (groundwater-filled boreholes) with the pumping flow rate is investigated over the whole 39-month-long period with daily resolution (Figure 26). Among all these 1170 days (from March 19th, 2018 to May 31st, 2021), the flow is laminar some 30% of the time, mostly during summer operation. Laminar flow regime inside the U-pipe (Reynolds number below 2300) can provoke a steeper exponential increase of daily R_b* up to 0.66 m.K/W (Figure 26). On the other hand, minimum flow rates in the range of 0.25 - 0.35 l/s per borehole can assure a turbulent regime and lower values for R_b*.

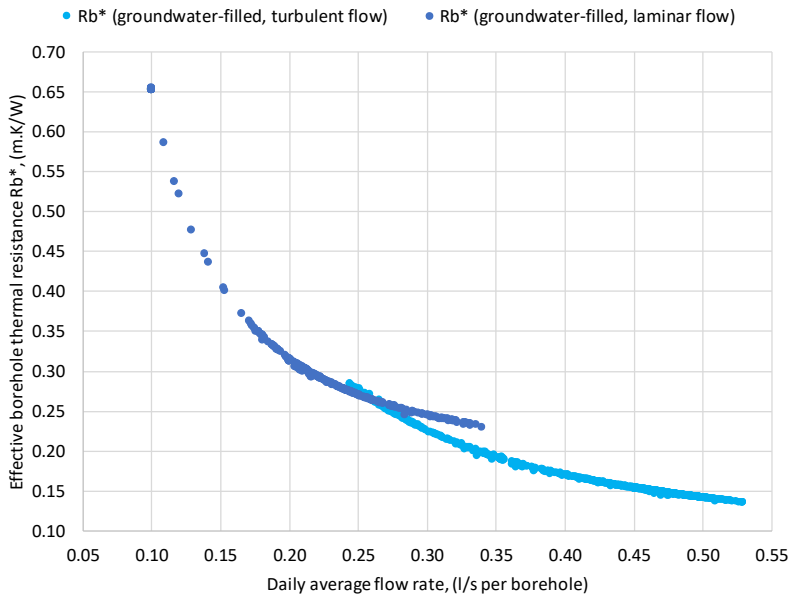

Figure 26. Effective thermal resistance of groundwater-filled boreholes vs. flow rate.

Moreover, it is acknowledged a significant variability of R_b* in real operation, considering that the initial TRT results estimated R_b* slightly below 0.1 m.K/W. Lower flow rate (laminar flow within the U-pipe) increases the thermal short-circuiting between both legs, rises the effective borehole thermal resistance and ultimately degrades the overall efficiency of the GHE (Javed and Spitler, 2016; Hellström, 2016).

4. Discussion

This dissertation analyses the practical aspects and proposes a hands-on approach for GSHP-ATES integration in both district heating and cooling networks (**Publications 1 and 2**). For this purpose, the GSHP-ATES system is evaluated in terms of technoeconomic feasibility, efficiency, and long-term impact on the aquifer.

Furthermore, Aalto University New Campus Complex – currently operating large-scale GSHP-BTES application - is investigated and monitored, as another topic of this dissertation in **Publications 3 and 4**.

The main outcomes and relevant practical achievements of the research will be discussed in this section, as well as their limitations and suggestions for future investigation and improvement.

4.1 Practical implications of the research

The analyzed ATES-related case studies were successful in demonstrating that using limited and uncertain data (regarding aquifer's hydrogeology), it is possible to holistically integrate (**Publication 1**) and mathematically model (**Publication 2**) GSHP-ATES system operation, as well as analyze with reasonable accuracy their performance efficiency, techno-economic feasibility and the impact of ATES operation on the surrounding groundwater areas.

The required heat pump capacity was chosen to cover the base load heat demand in **Publication 1** (domestic hot water demand, which in practice allows to switch off the peak boiler in summer), while in **Publication 2** the capacity was limited by the maximum daily ATES pumping flow rate (taken as annual average). Therefore, Pukkila case study (**Publication 1**), as heating dominated, is annually unbalanced (more heat is extracted from the ground than injected), thus requiring reversible ATES operation and warm / cold well doublet. The correct placement and distance between wells of opposite thermal type is essential for ensuring correct and efficient long-term operation. The normally applied rule of thumb for well distance – 3 times the average thermal radius – can be substantially decreased in urban areas to maximally reduce ATES GHG emissions. Beernink et al. (2022) concluded that for individual systems the optimal distance between wells is 0.5–1 times the average thermal radius for wells of the same thermal type and 2 times for opposite types. This important finding can

substantially contribute to ATES implementation and deployment in cities, where the available subsurface space is quite limited.

On the other hand, in Turku case study (**Publication 2**), GSHP-ATES system, balancing heating and cooling loads in a single process, allowed implementing the simpler one-way ATES operation with practically zero thermal influence on the aquifer. Moreover, the introduction of first stage cooling exchanger in Scenario 2, allowed more DH demand covered by the heat pump (+13%), more DC covered (+15%) and decreased the energy production cost by 5% (with the same ATES pumping flow rate, which is normally limited for the specific groundwater area).

In this respect, the future transition to low district heating networks (Guzzini et al., 2020) by the introduction of GSHP, can definitely benefit from the proposed mathematical methodology in **Publication 2** due to its capability to find a trade-off between the energy production cost, ATES pumping flow rate and the temperature drop introduced by the heat pump in DH supply line. **Publication 2**, although focused on the concrete Turku case study implementation, highlighted the versatility of such mathematical integration, since it can be deployed at different levels of DH/DC network: within a small/medium size branch of the network, like the Kupittaa district branch, or even within a district substation room of a single building. The severity of hot weather during recent summers due to climate change, even in Nordic latitudes (like the 2021 record heatwave experienced in Finland; Reuters, 2021), will increase the demand of district cooling in urban areas in the forthcoming decades. Turku case (**Publication 2**) clearly demonstrated major economic and technical improvements of GSHP-ATES implementation by dispatching annually balanced heating and cooling loads within integrated urban energy networks.

Publication 3 developed and implemented a novel data management methodology to assess the performance of a complex GSHP–BTES system (Aalto New Campus Complex). The data validation and reconciliation (DVR) procedure normally intends to correct measurement errors and can be expressed mathematically as an optimization problem for optimally correcting the measurement data in a way that the adjusted values are consistent with the laws of conservation (in this case both sides of the GSHP should be balanced). Application of the generalized DVR method, which handles raw measured data with unmeasured quantities (GSHP condenser and evaporator loads), tends to decrease the uncertainty after data reconciliation. The final goal of improving the quality of measured data is the assessment of GSHP performance indicators and the achievement of higher efficiency of the long-term GSHP-BTES operation. In practice, the proposed data management methodology in **Publication 3** is a versatile tool for achieving consistency and accuracy of measured data. Potentially, it can be applied to similar complex GSHP systems, simultaneously providing heating and cooling and utilizing various combinations of heat sources and sinks.

Publication 4 continued the investigation of Aalto New Campus Complex and more specifically focused on its BTES field. The accurate evaluation and modelling of the effective thermal resistance of groundwater-filled boreholes

(R_b*) is still challenging, as is the long-term simulation of the whole BTES field. The proposed methods are important steps in order to fill this gap. The implementation of working algorithm, specifically developed for R_b* update of groundwater-filled boreholes, and coupled with BTES-simulation tool, is a significant breakthrough for increasing the modeling accuracy of groundwater-filled-borehole fields.

4.2 Input data uncertainty and limitations

The presented ATES-related case studies (**Publications 1 and 2**) were carried out using quite limited and uncertain information regarding the hydrogeology of the studied groundwater areas. The fundamental assumptions - normally simplified during the prefeasibility phase - were that the aquifer layer is uniform, confined and isotropic in the considered area. For more accurate aquifer parameters estimation, additional geological survey and tests for non-equilibrium (transient) flow conditions should be conducted as next steps for groundwater model calibration and validation.

In **Publications 3**, the fundamental issues in the accuracy of all thermal energy meters motivated the development of an innovative methodology for measured data management. A specifically developed DVR methodology was utilized for adjusting the measured data for consistency, which mitigates the inherent uncertainty of the energy meters. Certain system limitations have also been detected for handling and enhancing the AHU free-cooling in summer operation, in practice creating a free-cooling bottleneck and limiting the utilization of the BTES resource up to around 11°C fluid temperature. Another design limitation of the GSHP-BTES energy system is the impossibility to recover the dissipation waste heat during summer operation, which would have mitigated the annual excessive heat extraction rate (1.7 GWh/a net heat extraction from the ground during the first annual evaluation period) and the potential BTES overcooling in the long-term.

In **Publications 4**, the proposed methods based on DTS vertical profiles, have certain limitations since the estimation of borehole annulus temperature needs to be indirectly inferred (not measured). The developed algorithm for R_b* estimation, based on the recently developed correlations for groundwater-filled boreholes, might present higher uncertainty with lower pumping flow rates. The correlations are also limited to groundwater-filled boreholes with low or inexistent groundwater advection and based on experimental data of Scandinavian boreholes.

4.3 Suggestions for future research and improvement

The research regarding the GSHP-ATES case studies (**Publications 1 and 2**) can be continued, for example in the following directions:

- Additional geological survey and slug & pumping tests in order to more accurately define all relevant aquifer parameters and improve groundwater model quality

- Research on integration of different energy sources, such as thermo-solar panels, PV/PV-T panels, industrial waste heat utilization, low enthalpy sources like sewage water, etc.
- More detailed study on how GSHP-ATES economic feasibility is affected by the fluctuation of energy prices, i.e., the volatility of electricity prices

Regarding **Publications 3**, accurate calibration of the energy meters and uncertainty analysis of their operation will be fundamental tasks to accomplish in future research. GSHP underperformance, especially in summer operation, is also acknowledged and the main reason seems to be the HP partial load operation. It would be important to improve the control strategy of each HP module increasing their capacity factor, especially during the summer and the transition seasons (with optimal capacity range between 25% and 60%). Additionally, the compensation curve of HP condenser supply temperature vs. ODA should be revised. Heat pump supply temperature was too high during the summer of 2021 and might be another possible reason for heat pump COP degradation in summer operation.

Additionally, the BTES pumping flow rate should be controlled not only to meet the demand (heating demand in winter and space-cooling in summer), but also to guarantee the efficient heat transfer of the borehole exchanger (**Publication 4**). Minimum flow rate control strategy should be implemented in order to assure turbulent regime within the borehole U-pipe, especially in summer operation, when most of the days the circulation pumps operate sub-optimally. Furthermore, DTS measurements of groundwater temperature along the annulus space and the borehole wall (in addition to fluid temperature) are also recommendable since they are essential for improving the confidence and accuracy of the results.

5. Conclusions

Overall, all the case studies analyzed in this dissertation support the main argument of the research: GSHP and UTES are key vectors for decarbonization of heating and cooling networks. This tandem is especially effective when applied in a centralized way (Zhang et al. 2020) and very important for increasing the flexibility of the existing energy systems (Paiho et al., 2018). The main outcomes and findings of the present dissertation are summarized in Table 17.

Table 17. Research questions and main findings.

Research questions		Main outcomes and findings
RQ1	Is it possible to adequately integrate GSHP-ATES within the existing district heating and cooling networks?	Yes, it is, and the possible outcome is case dependent. **Publication 1** addresses the integration utilizing reversible ATES operation with warm and cold well doublet. **Publication 2** uses one-way quasi-isothermal ATES operation for balancing the heating and cooling loads.
RQ2	How can be assessed the energy system's efficiency and techno-economic feasibility?	**Publications 1 and 2** highlight that the capability to cover heating and cooling loads in a single process is essential for efficient GSHP-ATES operation. Both publications argue that the technological adequacy of GSHP-ATES implementation is also economically feasible, presenting a competitive energy production cost.
RQ3	What is the GSHP-ATES long-term impact on the aquifer?	A groundwater model is fundamental for the evaluation of this influence, in order to ensure sustainable and efficient long-term operation. **Publication 1** addresses the estimation of both hydraulic and thermal long-term impact on the aquifer, while **Publication 2** analyses only the hydraulic impact. Both publications propose a hands-on approach for this assessment using various available data sources.
RQ4	What are the challenges in retrieving and managing data from a complex GSHP-BTES system?	The main challenges are the accuracy and consistency of measured data. The proposed approach of **Publication 3** tackles these fundamental issues, decreases the overall uncertainty and enables the accurate estimation of the GSHP long-term performance indicators.
RQ5	How can relevant indicators be utilized for analyzing and improving the long-term system performance?	Performance indicators like heat pump COP, heating and cooling SPF, EFT, etc. are fundamental for characterizing the GSHP-BTES operation (**Publication 3**). Additionally, the COP dependence on EFT, ODA, and partial load operation are analyzed proposing concrete measures for system improvement.
RQ6	How the effective thermal resistance of groundwater-filled boreholes can be evaluated in real operation?	**Publication 4** proposes several approaches for this evaluation, utilizing measured data regarding boreholes' temperatures, flow rates and loads. One of the approaches utilizes the DTS temperature profile and various discretization methods, while the other approach develops a specific algorithm coupled with GHE simulation toolbox.
RQ7	Why appropriate modeling of groundwater-filled boreholes is crucial for a reliable long-term simulation?	Normally, GHE simulation tools can handle only grouted boreholes. **Publication 4** intends to fill this gap and concludes that the specifically developed algorithm for modeling of groundwater-filled boreholes is essential for an accurate and reliable long-term simulation.

5.1 GSHP-ATES integration within existing energy networks

The dissertation was successful in demonstrating and developing a holistic GSHP-ATES integration (**Publication 1**) and mathematical modeling for system's management (**Publication 2**): calculation of GSHP recirculation flow, estimation of heat pump COP, as well as an algorithm for computation of ATES pumping flow rate based on the capacity to cover heating and cooling demand in a single process. Additionally, system's technoeconomic feasibility, efficiency and the impact of GSHP-ATES operation on the nearby aquifer were evaluated. Groundwater model was developed and calibrated, utilizing different available data sources like the National Land Survey of Finland, Finnish Environment Institute and Geological Survey of Finland, as well as computational and modelling tools like MS Excel, QGIS and ModelMuse (MODFLOW).

The dispatch of combined heating and cooling loads using annual data of existing Finnish urban district was used in tandem with GSHP-ATES model. It presented attractive economic outcome – competitive energy production cost around 40 €/MWh (**Publication 1**) and 30 €/MWh (**Publication 2**), far below 79.11 €/MWh, which is the weighted average DH price in Finland (DH, 2018), as well as had very limited long-term impact on the nearby aquifer.

Overall, ATES-GSHP tandem proved to be a sustainable and effective alternative to the conventional thermal energy generation primarily based on fossil fuels. It is acknowledged the efficiency of ATES-GSHP systems due to their ability to recycle heating & cooling loads, using the subsurface as thermal storage within integrated district energy networks, especially effective in urban areas.

5.2 Measured performance of large-scale GSHP-BTES system

In **Publication 3**, the presented novel methodology for measured data management of a sophisticated GSHP–BTES energy system such as Aalto New Campus Complex was proven to be indispensable for overcoming the fundamental issues related to the inherent uncertainty of all thermal energy meters. The proposed approach was certainly essential for the accuracy and confidence of the final results and contributed to estimation of the principal GSHP long-term performance indicators of the energy system. The results of all loads on both sides of GSHP (evaporator and condenser) were reported and analyzed for the entire 18-month period, as were HP fluid temperatures, COP, and SPF (for system boundary 2). The HP COP, heating SPF (H2), cooling SPF (C2), and combined SPF (HC2) for the entire period are 3.7, 3.5, 9.3, and 4.0, respectively.

During the initial period for system evaluation (October 2019–September 2020), the corresponding values for HP COP, heating SPF (H2), cooling SPF (C2), and combined SPF (HC2) are 3.7, 3.5, 9.3, and 3.9, respectively. The huge imbalance ratio of 7.5 between the annual heat extracted from and injected into the ground is acknowledged. This can potentially affect the sustainable and safe GSHP–BTES operation in the long-term (excessive cooling of the BTES field).

Additionally, the initial evaluation period was analyzed more thoroughly in terms of heat pump efficiency, i.e., COP dependence on EFT, ODA, and partial load operation. It was detected lower measured heat pump COP in summer operation, much lower than the calculated (expected) Lorentz/Carnot COP. A closer analysis of HP partial load operation revealed that the heat pump COP drops sharply for an average HP capacity below 25%, which mostly corresponds to summer operation. This drop might also be associated with the increase in parasitic loads at the beginning and end of the summer (daily ODA between 14 and 20 °C) and the transition periods (daily ODA between 12 and 15 °C) when the GSHP has to supply intermittent AHU-cooling loads with more frequent starts and stops. In any case, the detected HP underperformance in summer should be additionally investigated and corrected.

5.3 Groundwater-filled boreholes and BTES field modeling

Publication 4 introduced several approaches for determining the effective thermal resistance R_b^* of groundwater-filled boreholes. The proposed two methods utilized the DTS temperature profile of one representative borehole of the irregular BTES field, derived the borehole annulus temperature based on fluid inlet, bottom, and outlet temperatures and introduced different methodologies for discretizing and modeling the vertical profile in order to fit the DTS measurements. The first method estimates the fluid-water LMTD and the fluid-to-water heat transfer coefficient. The second method utilizes the borehole wall temperature and is based on Hellström's formulation of borehole vertical profile. The final goal of both methods is the derivation of R_b^*.

The second approach of **Publication 4** utilizes the recently developed correlations for groundwater-filled boreholes. The resulting algorithm for the effective thermal resistance R_b^* of groundwater-filled boreholes is implemented within the python-based toolbox for GHE simulation *Pygfunction*.

A simulation of the initial 39-months of system operation is conducted with *Pygfunction* and validated against measured data. One of the simulation scenarios is a hybrid model between *Pygfunction* and the algorithm implementation for groundwater-filled boreholes, updating R_b^* on a daily basis. The other three scenarios used grouted boreholes with specified grout thermal conductivity and constant borehole thermal resistance over the entire simulation. Overall, the hybrid model (with daily Rb^* update) presented the best indicators and fitted well with measurements. Therefore, it is concluded that the specifically developed algorithm for calculating the R_b^* of groundwater-filled boreholes is essential for a reliable long-term simulation of the BTES field.

References

Annex 52. (2021). Long term performance measurement of GSHP Systems serving commercial, institutional and multi-family buildings. Available online: https://heatpumpingtechnologies.org/annex52/ (accessed on 4 November 2021).

Bakr, M., van Oostrom, N., & Sommer, W. (2013). Efficiency of and interference among multiple Aquifer Thermal Energy Storage systems; A Dutch case study. *Renewable Energy*, 60, pp. 53-62. https://doi.org/10.1016/j.renene.2013.04.004

Bayer, P., Attard, G., Blum, P., & Menberg, K. (2019). The geothermal potential of cities. *Renewable and Sustainable Energy Reviews*, 106, pp. 17-30. https://doi.org/10.1016/j.rser.2019.02.019

Beernink, S., Bloemendal, M., Kleinlugtenbelt, R., Hartog, N. (2022). Maximizing the use of aquifer thermal energy storage systems in urban areas: effects on individual system primary energy use and overall GHG emissions. *Applied Energy*, 311, 118587, https://doi.org/10.1016/j.apenergy.2022.118587

Bell, I. (2021). CoolProp Documentation. Available online: https://buildmedia.readthedocs.org/media/pdf/coolprop/latest/coolprop.pdf (accessed on 7 July 2021).

Bloemendal, M., Olsthoorn, T., & Boons, F. (2014). How to achieve optimal and sustainable use of the subsurface for Aquifer Thermal Energy Storage. *Energy Policy*, 66, pp. 104-114. https://doi.org/10.1016/j.enpol.2013.11.034

Bloemendal, M., Olsthoorn, T., & van de Ven, F. (2015). Combining climatic and geohydrological preconditions as a method to determine world potential for aquifer thermal energy storage. *Science of the Total Environment*, 538, pp. 621-633. https://doi.org/10.1016/j.scitotenv.2015.07.084

Bloemendal, M., Jaxa-Rozen, M., & Olsthoorn, T. (2018). Methods for planning of ATES systems. *Applied Energy*, 216, pp. 534-557. https://doi.org/10.1016/j.apenergy.2018.02.068

Bockelmann, F. & Fisch, M. N. (2019). It Works—Long-Term Performance Measurement and Optimization of Six Ground Source Heat Pump Systems in Germany. Energies (Basel), 12(24). https://doi.org/10.3390/en12244691

Bonte, M., Stuyfzand, P. J., Hulsmann, A., & van Beelen, P. (2011). Underground thermal energy storage: Environmental risks and policy developments in the Netherlands and European Union. *Ecology and Society*, 16(1):22. https://doi.org/10.5751/ES-03762-160122

Bozkaya, B., Li, R., Labeodan, T., Kramer, R., & Zeiler, W. (2017). Development and evaluation of a building integrated aquifer thermal storage model. *Applied Thermal Engineering*, 126, pp. 620-629. https://doi.org/10.1016/j.applthermaleng.2017.07.195

BP. (2020). BP Energy Outlook 2020 Edition. Available online: https://www.bp.com/content/dam/bp/business-sites/en/global/corporate/pdfs/energy-economics/energy-outlook/bp-energy-outlook-2020.pdf (accessed on 13 January 2021).

Butler, D.; Abela, A.; Martin, C. (2016). Heat meter accuracy testing (UK Government, Department for Business, Energy & Industrial Strategy). Available online: https://assets.publishing.service.gov.uk/government/uploads/system/uploads/attachment_data/file/576680/Heat_Meter_Accuracy_Testing_Final_Report_16_Jun_incAnxG_for_publication.pdf (accessed on Jan 15, 2021).

Caljé, R.J. (2010). Future use of Aquifer Thermal Energy Storage below the historic center of Amsterdam. Master's Thesis, Delft University of Technology, Netherlands.

Christodoulides, P., Vieira, A., Lenart, S., Maranha, J., Vidmar, G., Popov, R., Georgiev, A., Aresti, L., & Florides, G. (2020). Reviewing the Modeling Aspects and Practices of Shallow Geothermal Energy Systems. *Energies (Basel)*, *13*(16), 4273. https://doi.org/10.3390/en13164273

Cimmino, M.; Thorne, D.; Langevin, C.D.; Sukop, M.C. (2018). Pygfunction: An Open-Source Toolbox for the Evaluation of Thermal Response Factors for Geothermal Borehole Fields. In Proceedings of the eSim 2018, the 10th conference of IBPSA, Montreal, QC, Canada, 28 May 2018; pp. 492–501, ISBN 978-2-921145-88-6.

Claesson, J. & Hellström, G. (2011). Multipole method to calculate borehole thermal resistances in a borehole heat exchanger. *HVAC&R Research*, 17(6), pp. 895–911. https://doi.org/10.1080/10789669.2011.609927

Connolly, D., Lund, H., Mathiesen, B. V., Werner, S., Möller, B., Persson, U., Boermans, T., Trier, D., Østergaard, P. A., & Nielsen, S. (2014). Heat Roadmap Europe: Combining district heating with heat savings to decarbonise the EU energy system. *Energy Policy*, 65, pp. 475–489. https://doi.org/10.1016/j.enpol.2013.10.035

DEA. (2020). Danish Energy Agency. Technology Data for Generation of Electricity and District Heating. Available online: https://ens.dk/en/our-services/projections-and-models/technology-data/technology-data-generation-electricity-and (accessed on Feb 17, 2020).

DH. (2018). Finnish Energy, District Heating in Finland 2018. Available online: https://energia.fi/files/4092/District_heating_in_Finland_2018.pdf (accessed 22.7.2020)

Drenkelfort, Kieseler, S., Pasemann, A., & Behrendt, F. (2014). Aquifer thermal energy storages as a cooling option for German data centers. Energy Efficiency, 8(2), pp. 385–402. https://doi.org/10.1007/s12053-014-9295-1

EC. (2016). Communication from the Commission to the European Parliament, the Council, the European Economic and Social Committee and the Committee of the Regions an eu Strategy on Heating and Cooling (COM/2016/051 final). Available online: https://eur-lex.europa.eu/legal-content/EN/TXT/?qid=1575551754568&uri=CELEX:52016DC0051 (accessed on 13 January 2021)

EED. (2021a). Earth Energy Designer (EED). Available online: https://buildingphysics.com/eed-2/ (accessed on 15 October 2021).

EED. (2021b). Tutorial examples for EED v4. Available online: https://buildingphysics.com/download/exampleseed.pdf (accessed on 15 July 2021).

EPBD. (2021). Proposal for a Directive of the European Parliament and the Council on the Energy Performance of Buildings (recast). Available online:

https://ec.europa.eu/energy/sites/default/files/proposal-recast-energy-performance-buildings-directive.pdf (accessed on 10 February 2022)

EU. (2018). Renewable Energy for Heating and Cooling (Eurostat report). Available online: https://ec.europa.eu/eurostat/web/products-eurostat-news/-/DDN-20200211-1?inheritRedirect=true&redirect=%2Feurostat%2F (accessed on 26 October 2021)

EUROHEAT. (2008). Guidelines for District Heating Substations, Approved by the Euroheat & Power Board.

Fahlén, P. (2012). Capacity control of heat pumps. REHVA Journal 05/2012. Available online: https://www.rehva.eu/rehva-journal/chapter/capacity-control-of-heat-pumps (accessed on 20 January 2022)

Fleuchaus, P., Godschalk, B., Stober, I., & Blum, P. (2018). Worldwide application of aquifer thermal energy storage – A review. *Renewable and Sustainable Energy Reviews*, 94, pp. 861-876. https://doi.org/10.1016/j.rser.2018.06.057

Fleuchaus, P., Schüppler, S., Godschalk, B., Bakema, G., Blum, P. (2020) Performance analysis of Aquifer Thermal Energy Storage (ATES), Renewable Energy, 146, pp. 1536-1548. https://doi.org/10.1016/j.renene.2019.07.030

Gehlin, S., Spitler, J. D. (2021). Half-term Results from IEA HPT Annex 52 - Long-term Performance Monitoring of Large GSHP Systems. In 13th IEA Heat Pump Conference, April 26-29, 2021 Jeju, Korea.

Greenpeace. (2020). Toxic air: The price of fossil fuels. Available online: https://www.greenpeace.org/usa/wp-content/uploads/2020/02/The-Price-of-Fossil-Fuels-media-briefing.pdf (accessed on 4 May 2020).

Grundfos. (2020a). Grundfos SP Submersible Pumps. Available online: https://www.grundfos.com/products/find-product/sp.html (accessed on 17 February 2020).

Grundfos. (2020b). Grundfos NB/NBG Centrifugal Pumps. Available online: https://www.grundfos.com/products/find-product/nb-nbg-nbe-nbge.html (accessed on 17 February 2020).

Gustafsson, A. & Westerlund, L. (2011). Heat extraction thermal response test in groundwater-filled borehole heat exchanger – Investigation of the borehole thermal resistance. *Renewable Energy*, *36*(9), pp. 2388–2394. https://doi.org/10.1016/j.renene.2010.12.023

Guzzini, A., Pellegrini, M., Pelliconi, E., Saccani, C. (2020). Low Temperature District Heating: An Expert Opinion Survey. Energies 13(4): 810. https://doi.org/10.3390/en13040810

Haehnlein, S., Bayer, P., & Blum, P. (2010). International legal status of the use of shallow geothermal energy. In Renewable and Sustainable Energy Reviews, 14(9), pp. 2611-2625. https://doi.org/10.1016/j.rser.2010.07.069

Harbaugh, Arlen, W. (2005). MODFLOW-2005, The U . S . Geological Survey Modular Ground-Water Model — the Ground-Water Flow Process. *U.S. Geological Survey Techniques and Methods 6-A15*. https://doi.org/10.3133/tm6A16

Hecht-Méndez, J., Molina-Giraldo, N., Blum, P., & Bayer, P. (2010a). Evaluating MT3DMS for heat transport simulation of closed geothermal systems. Ground Water, pp. 741-756. https://doi.org/10.1111/j.1745-6584.2010.00678.x

Hecht-Méndez, J.; Molina-Giraldo, N.; Blum, P.; Bayer, P. (2010b) Use of MT3DMS for Heat Transport Simulation of Shallow Geothermal Systems, Proceedings World Geothermal Congress, Bali, Indonesia, 25-29 April 2010

Hellström, G. (2016). Thermal performance of borehole heat exchangers. *Energy Convers. Manag*. 2016, 122, pp. 544–551.

Hooimeijer, F. L., & Maring, L. (2018). The significance of the subsurface in urban renewal. *Journal of Urbanism*, 11(3), pp. 303-328. https://doi.org/10.1080/17549175.2017.1422532

Hoving, J., Bozkaya, B., Zeiler, W., Haan, J. F., Boxem, G., & Velden, van der, J. A. J. (2014). Thermal storage capacity control of aquifer systems. In BauSim 2014, 22-24 September 2014, Aachen, Germany (pp. 617-625)

HPT. (2020). Heat Pumping Technologies MAGAZINE-Integration of Heat Pumps into the Future Energy System. Available online: https://issuu.com/hptmagazine/docs/hpt_magazine_no1_2020 (accessed on 25 January 2021).

IEA. (2021). Net Zero by 2050: A Roadmap for the Global Energy Sector, International Energy Agency (Special Report). Available online: https://iea.blob.core.windows.net/assets/4719e321-6d3d-41a2-bd6b-461ad2f850a8/NetZeroby2050-ARoadmapfortheGlobalEnergySector.pdf (accessed on 23 August 2021).

Incropera, F.P. (2007). Fundamentals of Heat and Mass Transfer, 6th ed.; John Wiley & Sons, Inc.: Hoboken, NJ, USA, 2007; Volume 1, ISBN 9780471457282.

Javed, S.; Nakos, H.; Claesson, J. (2012). A method to evaluate thermal response tests on groundwater-filled boreholes. *ASHRAE Trans*. 2012, 118, pp. 540–549.

Javed, S.; Claesson, J. (2017). Second-order multipole formulas for thermal resistance of single u-tube borehole heat exchangers. In Proceedings of the IGSHPA Technical/Research Conference and Expo 2017, Denver, CO, USA, 14–16 March 2017.

Javed, S.; Spitler, J. (2016). Calculation of Borehole Thermal Resistance; Woodhead Publishing: Cambridge, UK, 2016; Volume 1, ISBN 9780081003220.

Johnsson, J. & Adl-Zarrabi, B. (2019). Modelling and evaluation of groundwater filled boreholes subjected to natural convection. *Applied Energy*, *253*, 113555. https://doi.org/10.1016/j.apenergy.2019.113555

Kallio, J. (2019). Geothermal Energy Use, Country Update for Finland. Available online: http://europeangeothermalcongress.eu/wp-content/uploads/2019/07/CUR-10-Finland.pdf (accessed on 11 December 2020).

Lamarche, L., Raymond, J., & Koubikana Pambou, C. (2017). Evaluation of the Internal and Borehole Resistances during Thermal Response Tests and Impact on Ground Heat Exchanger Design. *Energies (Basel)*, *11*(1), 38. https://doi.org/10.3390/en11010038

Lu, H., Tian, P., & He, L. (2019). Evaluating the global potential of aquifer thermal energy storage and determining the potential worldwide hotspots driven by socio-economic, geo-hydrologic and climatic conditions. *Renewable and Sustainable Energy Reviews*, 112, pp. 788-796. https://doi.org/10.1016/j.rser.2019.06.013

Lund, J. W., & Toth, A. N. (2020). Direct utilization of geothermal energy 2020 worldwide review. *Geothermics*, 101915. https://doi.org/10.1016/j.geothermics.2020.101915

Luo, J., Rohn, J., Bayer, M., Priess, A., Wilkmann, L., & Xiang, W. (2015). Heating and cooling performance analysis of a ground source heat pump system in Southern Germany. Geothermics, 53, 57–66. https://doi.org/10.1016/j.geothermics.2014.04.004

ModelMuse. (2022). ModelMuse: A Graphical User Interface for Groundwater Models. Available online: https://www.usgs.gov/software/modelmuse-graphical-user-interface-groundwater-models (accessed on Jan 17, 2022).

Naicker, S. S., & Rees, S. J. (2018). Performance analysis of a large geothermal heating and cooling system. *Renewable Energy*, 122, pp. 429–442. https://doi.org/10.1016/j.renene.2018.01.099

Nielsen, & Möller, B. (2013). GIS based analysis of future district heating potential in Denmark. Energy (Oxford), 57, pp. 458–468. https://doi.org/10.1016/j.energy.2013.05.041

NLSF. (2020). National Land Survey of Finland Available online: https://tiedostopalvelu.maanmittauslaitos.fi/tp/kartta?lang=en (accessed on Apr 14, 2020).

Nordman, R. (2012). Seasonal Performance factor and Monitoring for heat pump systems in the building sector, SEPEMO-Build, Final Report. Intelligent Energy Europe.

NORDPOOL. (2020). Nordpool Finnish day-ahead monthly prices 2006-2020. Available online: https://www.nordpoolgroup.com/Market-data1/Dayahead/Area-Prices/FI/Monthly/?dd=FI&view=table (accessed on Mar 16, 2020).

Paiho, S., Saastamoinen, H., Hakkarainen, E., Similä, L., Pasonen, R., Ikäheimo, J., Horsmanheimo, S. (2018). Increasing flexibility of Finnish energy systems—A review of potential technologies and means. *Sustainable Cities and Society*, 43, pp. 509-523. https://doi.org/10.1016/j.scs.2018.09.015

Piechurski, K., Szulgowska-Zgrzywa, M., & Danielewicz, J. (2017). The impact of the work under partial load on the energy efficiency of an air-to-water heat pump. E3S Web of Conferences, 17. https://doi.org/10.1051/e3sconf/20171700072

Pellegrini, M., Bloemendal, M., Hoekstra, N., Spaak, G., Andreu Gallego, A., Rodriguez Comins, J., Steeman, H. (2019). Low carbon heating and cooling by combining various technologies with Aquifer Thermal Energy Storage. *Science of the Total Environment*, 665, pp. 1-10. https://doi.org/10.1016/j.scitotenv.2019.01.135

Pero, J. (2016) District heating business development in Mäntsälän Sähkö limited company. Available online: http://lutpub.lut.fi/bitstream/handle/10024/123395/diplomityo_pero_juha.pdf (accessed 24.5.2019)

Popovski, E., Aydemir, A., Fleiter, T., Bellstädt, D., Büchele, R. & Steinbach, J. (2019). The role and costs of large-scale heat pumps in decarbonising existing district heating networks – A case study for the city of Herten in Germany. *Energy*, 180, pp. 918-933. https://doi.org/10.1016/j.energy.2019.05.122

QGIS. (2020). QGIS - The Leading Open Source Desktop GIS. Available online: https://www.qgis.org/en/site/about/index.html (accessed on Mar 12, 2020).

Reinholdt, L.; Kristófersson, J.; Zühlsdorf, B.; Elmegaard, B.; Jensen, J.; Ommen, T.; Jørgensen, P.H. (2018). Heat pump COP, part 1: Generalized method for screening of system integration potentials. In Proceedings of the Refrigeration Science and Technology, Valencia, Spain, 18–20 June 2018.

Reuters. (2021). Finland on course for record hot summer as heatwave stifles Nordic region. Available online: https://www.reuters.com/world/europe/finland-course-record-hot-summer-heatwave-stifles-nordic-region-2021-07-09/ (accessed on 2 February 2022).

Romera, J.J.G. (2021). Iapws Documentation. Available online: https://iapws.readthedocs.io/_/downloads/en/latest/pdf/ (accessed on 7 July 2021).

Schmidt, T., Pauschinger, T., Sørensen, P.A., Snijders, A., Thornton, J. (2018) Design Aspects for Large-scale Pit and Aquifer Thermal Energy Storage for District Heating and Cooling. *Energy Procedia*, 149, pp. 585-594. https://doi.org/10.1016/j.egypro.2018.08.223

Schüppler, S., Fleuchaus, P., & Blum, P. (2019). Techno-economic and environmental analysis of an Aquifer Thermal Energy Storage (ATES) in Germany. Geothermal Energy (Heidelberg), 7(1), pp.1–24. https://doi.org/10.1186/s40517-019-0127-6

Soltani, M., M. Kashkooli, F., Dehghani-Sanij, A., Kazemi, A., Bordbar, N., Farshchi, M., . . . B. Dusseault, M. (2019). A comprehensive study of geothermal heating

and cooling systems. *Sustainable Cities and Society*, 44, pp. 793-818. https://doi.org/10.1016/j.scs.2018.09.036

Sommer, W., Valstar, J., Leusbrock, I., Grotenhuis, T., & Rijnaarts, H. (2015). Optimization and spatial pattern of large-scale aquifer thermal energy storage. *Applied Energy*, 137, pp. 322-337. https://doi.org/10.1016/j.apenergy.2014.10.019

Spitler, J., & Gehlin, S. (2015). Thermal response testing for ground source heat pump systems—An historical review. *Renewable & Sustainable Energy Reviews*, *50*, pp. 1125–1137. https://doi.org/10.1016/j.rser.2015.05.061

Spitler, J., & Gehlin, S. (2019). Measured performance of a mixed-use commercial-building ground source heat pump system in Sweden. *Energies*, 12(10). https://doi.org/10.3390/en12102020

Spitler, J., Javed, S., & Ramstad, R. K. (2016a). Natural convection in groundwater-filled boreholes used as ground heat exchangers. *Applied Energy*, 164, pp. 352–365. https://doi.org/10.1016/j.apenergy.2015.11.041

Spitler, J.; Javed, S.; Grundmann, R. (2016b). Calculation Tool for Effective Borehole Thermal Resistance. In Proceedings of the 12th REHVA World Congress, Aalborg, Denmark, May 22 – 25, 2016

SYKE. (2020). Finnish Environment Institute / Suomen Ympäristökeskus. Available online: https://www.syke.fi/en (accessed on Apr 14, 2020).

Todorov, O., Alanne, K., Virtanen, M. & Kosonen, R. (2020). A novel modelling approach of ground source heat pump application for district heating and cooling, developed for a case study of an urban district in Finland, *BuildSim Nordic Conference* 2020, Oslo, October 13, Session 1: District Heating and Large Buildings; SINTEF Academic Press, ISBN 978-82-536-1679-7 (pdf). Available online: https://sintef.brage.unit.no/sintef-xmlui/bitstream/handle/11250/2683219/Pages%20from%20SProceedings%20no%205-39.pdf?sequence=1 (accessed on Jan 20, 2022).

Todorov, O., Vallin, S., Virtanen, M., Leppäharju, N. (2021). Case study report for monitoring project – Aalto University New Campus Complex, Otaniemi (Espoo). Finland. IEA HPT Annex 52 – Long-term performance monitoring of GSHP systems serving commercial, institutional and multi-family buildings. https://doi.org/10.23697/cm70-g204

Tuominen, P., Holopainen, R., Eskola, L., Jokisalo, J., & Airaksinen, M. (2014). Calculation method and tool for assessing energy consumption in the building stock. Building and Environment, pp. 153-160. https://doi.org/10.1016/j.buildenv.2014.02.001

WATANABE, C., OHASHI, E., HIROTA, M., NAGAMATSU, K., & NAKAYAMA, H. (2009). Evaluation of Annual Performance of Multi-type Air-conditioners for Buildings. Journal of Thermal Science and Technology (Japan Society of Mechanical Engineers), 4(4), pp. 483–493. https://doi.org/10.1299/jtst.4.483

WEF. (2022). The Global Risks Report 2022, 17th Edition, World Economic Forum. Available online: https://www3.weforum.org/docs/WEF_The_Global_Risks_Report_2022.pdf (accessed on Feb 1, 2022).

YLE. (2021). Finland experiencing mildest winter in 100 years. Available online: https://yle.fi/uutiset/osasto/news/finland_experiencing_mildest_winter_in_100_years/11160303 (accessed on Jan 18, 2021).

Zheng, C., & Wang, P. P. (1999). MT3DMS: A Modular Three-Dimensional Multispecies Transport Model for Simulation of Advection, Dispersion and Chemical Reactions of Contaminants in Groundwater Systems; Documentation and User's

Guide. Contract Report SERDP-99-1, US Army Corps of Engineers, Engineer Research and Development Center, 220.

Zhang, Y., Qi, H., Zhou, Y., Zhang, Z., & Wang, X. (2020). Exploring the impact of a district sharing strategy on application capacity and carbon emissions for heating and cooling with GSHP systems. *Applied Sciences*, 10(16):5543. https://doi.org/10.3390/app10165543

Climate change, exacerbated by the increasing greenhouse gas emissions (GHG), has abruptly altered the life on Earth during the last few decades. Extreme weather, scarcity of fuels and natural resources, proliferating social inequalities and conflicts, are symptoms that the situation is getting out of hand. In this context, our energy systems, still dominated by the utilization of fossil fuels, are responsible for high emissions and air pollution, especially in cities. The decarbonization of heating and cooling networks is a priority, and ground-source heat pumps (GSHP) combined with underground thermal energy storage (UTES) offer an attractive technology to match supply and demand, allowing efficient integration of renewable energy sources and waste heat recycling.

Aalto-DT 66/2022

ISBN 978-952-64-0798-2 (printed)
ISBN 978-952-64-0799-9 (pdf)
ISSN 1799-4934 (printed)
ISSN 1799-4942 (pdf)

Aalto University
School of Engineering
Department of Mechanical Engineering
www.aalto.fi

BUSINESS + ECONOMY

ART + DESIGN + ARCHITECTURE

SCIENCE + TECHNOLOGY

CROSSOVER

DOCTORAL THESES